EVOLUTION OF PERINE MORPHOLOGY IN THE THELYPTERIDACEAE

Nikisha Patel,[1],*,†,‡ Susan Fawcett,* Michael Sundue,* and Jessica M. Budke†

*Pringle Herbarium, Department of Plant Biology, University of Vermont, Burlington, Vermont 05401, USA; †Department of Ecology
and Evolutionary Biology, University of Tennessee, Knoxville, Tennessee 37996, USA; and ‡Department of Ecology
and Evolutionary Biology, University of Connecticut, Storrs, Connecticut 06269, USA

Editor: Steffi Ickert-Bond

Premise of research. Spores and pollen often exhibit distinctive morphology, resulting from the structure of the exine (spore wall), and elaborate external ornamentation, known as perine. Spore-dispersed plants, particularly ferns, exhibit remarkable variation in the surface structure of their spores and provide an excellent model for the study of morphological trait evolution. Our goal is to assess the utility of spore morphology for characterizing clades and taxa. For this study, we chose Thelypteridaceae, a family of ferns with over 1000 species and exceptionally diverse spore morphology.

Methodology. We generated a 200-species molecular phylogeny representing family diversity. We assigned discrete states for seven morphological characters of spores based on images from scanning electron microscopy (SEM). We then optimized these seven characters and their states on our molecular phylogeny, which represented about 10% of the species diversity in the family, including members of all 27 currently recognized genera, with the exception of the monotypic *Menisorus* and *Nannothelypteris*, which includes three species. We quantify phylogenetic signal and homoplasy for morphological traits and test for pairwise correlated evolution of traits. Finally, we provide a synoptic description of spore morphology for genera in the family, synthesizing our current findings with previous work.

Pivotal results. Reticulate perine and perforate perine, which show high phylogenetic signal and low homoplasy, characterized genera and major clades. Microstructure, or fine superficial sculpturing, was not synapomorphic for any group and varied at fine phylogenetic scales. Certain genera, such as *Amauropelta* and *Stegnogramma*, exhibit uniform morphology among their species, whereas others, such as *Christella*, are highly variable. Our phylogenetic analyses indicate that *Christella* and *Pronephrium* are nonmonophyletic, whereas infrageneric sections of these genera are largely corroborated.

Conclusions. Characters pertaining to perine macrostructure and perforations, in particular, were reconstructed as synapomorphic for genera or sections in the Thelypteridaceae. High variability of perine characters within the christelloid clade suggests that it is a promising group on which to focus further sampling. Our approach provides explicit statements of character evolution for perine morphology that can be used as a framework for further studies. We demonstrated that the repository of high-quality SEM images of spores in the literature serves as a rich source of morphological data.

Keywords: character state reconstruction, ferns, perispore, phylogenetics, spores.

Online enhancements: appendix figures and tables, supplementary appendixes.

Introduction

Spores and pollen are critical to the dispersal and reproduction of land plants, and spores were crucial adaptations for the colonization of terrestrial environments (Kenrick and Crane 1997). Both spores and pollen often feature elaborate external ornamentation, composed of sporopollenin, surrounding the spore or pollen wall that is typically variable across taxonomic groups and is broadly referred to as perine or perispore (Wallace et al. 2011). Variation in perine morphology in pollen has been well studied in an evolutionary context (Bolick 1978; Crepet 1996; Wang et al. 2003; Furness and Rudall 2004). The type of pollen ornamentation in a taxon frequently corresponds to pollination syndrome—for example, echinate pollen characterizes entomophily and smooth pollen characterizes anemophily (Ferguson and Harley 1993; Ackerman 2000)—and pollen ornamentation has been a major source of taxonomic information (Poole and Hunt 1980; Ferguson 1984; Kosenko 1999). Spores, in contrast, are less well studied than pollen. Moss spores lack variation in ornamentation but are often used as indicators of

[1] Author for correspondence; email: nikisha.patel@uconn.edu.

polyploidy on the basis of size (Vaarama 1953; Paolillo and Kass 1977; Carrión et al. 1995). Species of the lycophyte genus *Isoëtes* feature elaborate spore ornamentation that is often diagnostic for species (Kott and Britton 1983; Hickey 1986). Spores and pollen are remarkably well preserved in the fossil record relative to other plant tissues, likely as a result of the chemical nature of sporopollenin, which is highly resistant to mechanical and chemical degradation (Van Bergen et al. 1995; Bernard et al. 2007). Improving our understanding of spore morphology in an evolutionary context for extant taxa may improve our ability to discern evolutionary patterns from fossil evidence for extinct taxa (Schneider et al. 2016).

Laesurae are the markings on a spore resulting from attachment to other spores borne either in a tetrad, resulting in trilete spores, or in a diad, resulting in monolete spores. These two character states provide the fundamental structural variation of fern spores (Wagner 1974). Transitions between the two types are infrequent, and the states often define major fern lineages. For instance, tetrahedral trilete spores are common in early-divergent leptosporangiate lineages (Cyatheales, Gleicheniales, Hymenophyllales, Osmundales), and monolete spores and trilete spores are each diagnostic for certain clades of Polypodiales as well (Brown 1960; Kramer and Green 1990). Spores vary in color—green, yellow, brown, black, tan, or white—and coloration is a combination of the perine and the storage materials of the spore (Lloyd and Klekowski 1970; Sundue et al. 2011). In terms of ornamentation, fern spore perine may be closely appressed or loosely attached to the spore wall, and a loosely attached perine is a synapomorphy for all eupolypod ferns (Schneider et al. 2016).

Perine morphology is highly variable among ferns (Tryon and Tryon 1982; Tryon and Lugardon 1991). Owing to this great variation, many species have been imaged using scanning electron microscopy (SEM), and the perine morphology has been considered in taxonomic studies (Wagner 1974; Puttock and Quinn 1980; Tryon and Tryon 1982; Moy 1988; Tryon and Lugardon 1991; Burrows 1997; Dai et al. 2002; Regalado and Sanchez 2002; Moran et al. 2007, 2010; Smith et al. 2008; Vasco et al. 2009; Wei and Dong 2012; Shah et al. 2019). However, only a few studies have examined the evolution of perine morphology in a phylogenetic context (Moran et al. 2007, 2010; Chao and Huang 2018). Using perine morphology, Moran et al. (2010) recovered synapomorphies for clades of bolbitidoid (Dryopteridaceae) ferns, and Moran et al. (2018) found similar results for genera of Blechnaceae.

Thelypteridaceae Ching ex Pic. Serm. is one of the most species-rich fern families, with approximately 1034 species (Smith et al. 2006; PPG I 2016) and spore ornamentation that varies at coarse scales (macrostructure) with broad folds, thin crests, echinae, or reticulation and at fine scales (microstructure) with spiculae, verrucae, or minute crests or folds (Wood 1973; Tryon and Lugardon 1991). Generic circumscription within the family has varied widely, with treatments ranging from only one (Morton 1963) to as many as 32 genera (Pichi Sermolli 1977). Recent molecular phylogenetic studies have improved resolution in the Thelypteridaceae, although taxonomic issues remain (Smith and Cranfill 2002; He and Zhang 2012; Almeida et al. 2016). Previous work on perine morphology in the Thelypteridaceae has included systematic monographs (Holttum 1971; Smith 1971; Wood 1973; Grimes 1980; Smith 1980; Tryon and Tryon 1982;

Tryon and Lugardon 1991; Dai et al. 2002, 2005; Alvarez-Fuentes 2010; Wang and Dai 2010) and spore atlases (Zhang 1976, 1990; Huang 1981; Mitui 1982; Ferrarini et al. 1986; Joaquin and Zamora 1996; Moon and Sun 2008; Shah et al. 2019). In addition, Wood (1973) and Wang and Dai (2010) each proposed classification for the Thelypteridaceae genera based on perine morphology.

The goal of the present work is to examine character evolution of spore ornamentation in the Thelypteridaceae. By optimizing multiple discrete characters from SEM spore images onto a molecular phylogeny representing 10% of the family diversity, we assess how well those traits correspond to monophyletic clades and taxonomic concepts. We quantify homoplasy and phylogenetic signal and test for pairwise correlation of character states in formal analyses that can inform future phylogenetic studies of spore and pollen morphology.

Methods

DNA Extraction, Amplification, and Sequencing

Eleven DNA sequences representing 11 species using three markers were generated from herbarium specimens vouchered at the Pringle Herbarium (VT; app. S1; apps. S1, S2 are available online). Total genomic DNA was extracted from fresh (1 g) or silica-dried (0.5 g) leaves using a cetyltrimethylammonium bromide procedure (Porebski et al. 1997). The plastid DNA sequences *rbcL*, *trnL-trnF* spacer region, and *matK* were polymeric chain reaction (PCR) amplified using previously published primers, with modifications for *rbcL* (Taberlet et al. 1991; Little and Barrington 2003; Rothfels et al. 2012). Markers *rbcL* and *trnL-trnF* were amplified using an initial denaturation step of 94°C for 10 min, followed by 35 cycles of 94°C for 45 s, 58°C for 1 min, and 72°C for 1 min. The marker *matK* was amplified using an initial denaturation step of 94°C for 3 min, followed by 30 cycles of 94°C for 45 s, 53°C for 45 s, and 72°C for 2 min and a final extension at 72°C for 10 min. Resulting PCR products were cleaned using ExoSAP-IT (USB, Cleveland, OH) and sequenced on an ABI PRISM 3730x automated sequencer (Genewiz Genomics, Danvers, MA). Each region was sequenced in both forward and reverse directions using the amplification primers.

Thelypteridaceae Supermatrix Assembly

The molecular matrix was constructed using the SUMAC package in Python (Freyman 2015). The GenBank database PLN (plant and fungal sequences) was downloaded to a local hard drive and searched using the algorithms UCLUST and USEARCH (Edgar 2010), which build a matrix through exploratory clustering of GenBank data within a chosen taxon. Thelypteridaceae was set as the taxonomic ingroup with no outgroup designated because the monophyly of the family is well established and the family can be rooted using its two sister subfamilies: Phegopteridoideae and Thelypteridoideae (He and Zhang 2012; Almeida et al. 2016). SUMAC also calculates missing sequence decisiveness scores (MSDS), which is a metric for determining the degree to which missing data would contribute to the decisiveness of the matrix if it were included. The newly

generated sequences were aligned to this matrix using MAFFT version 7.309 in Geneious version 10.0.9 (http://www.geneious.com; Kearse et al. 2012) and concatenated by taxon, creating chimeric operational taxonomic units that represent more than one specimen. The matrix included three nuclear and eight plastid markers (*atpA*, *atpB*, *LEAFY*, *NEO*, *matK*, *pgiC*, *psbA-trnH*, *rbcL*, *rps4-trnS*, *trnG-trnR*, and *trnL-trnF*). Each genetic marker was represented by at least five species, while each species was represented by at least two genetic markers (fig. A1; figs. A1, A2 are available online). The taxonomy was updated in accordance with PPG I (2016), and the alignment was edited manually as needed. Sequences that were suspected to be labeled with an incorrect species name were removed based on incongruities among single-gene trees and BLAST results. Although this approach leads to the assembly of a matrix with a large amount of missing data, previous studies indicate that phylogenetic analyses are robust to this shortcoming (Wiens and Morrill 2011).

Molecular Phylogenetic Analyses

Newly generated sequences were trimmed and assembled in Geneious version 9.1.1 (Kearse et al. 2012) and incorporated into the SUMAC matrix by aligning to individual markers using MAFFT (Katoh et al. 2017). Phylogenies were inferred using both maximum likelihood (ML) and Bayesian inference (BI), implemented through the CIPRES Science Gateway (Miller et al. 2010). Before analysis, PartitionFinder2 (Lanfear et al. 2016) was used to determine the optimal models for molecular evolution for each gene region and codon position. We used the rcluster algorithm within PartitionFinder2 (Stamatakis 2014; Lanfear et al. 2016), which recovered 15 partitions for our data set, each using either GTR+I+G or GTR+G. The ML analysis was performed using RAxML (Stamatakis 2014), designating the members of the Phegopteridoideae as the outgroup, and using the GTR model for each of the 15 partitions because of the restrictions in the models for ML analyses implemented in RAxML. BI was implemented in MRBAYES version 3.2.6 (Huelsenbeck and Ronquist 2001), using the 15 partitions and the optimal models recovered by PartitionFinder2 for two runs of 50,000,000 Markov chain Monte Carlo generations each that were sampled every 1000 generations with the first 25% of samples discarded as burn-in. Tracer version 1.6.0 (Rambaut et al. 2015) was used to check that effective sample sizes exceeded recommended minima (>200) and that the two runs converged.

Taxon Sampling for Spore Images

In total, 165 SEM spore images representing 118 species were scored for perine morphological characters. Of these, 49 images were newly generated for the study (sampled from specimens at VT and TENN), and 115 images were obtained from the literature (app. S1). The majority of newly imaged species are represented by a single specimen, but more than one specimen was imaged for five species. The DNA sequence and spore morphology data were not based on the same specimen in most cases. Five of the 30 genera sampled are represented in the optimization by previously published spore images exclusively (app. S1). To illustrate the morphological diversity in these

genera, we have generated new high-resolution images from representative species that were not included in the perine character optimization because of a lack of DNA data (figs. 1–6).

Scanning Electron Microscopy

Using a dissecting needle, spores were transferred from herbarium specimens to aluminum stubs (Zeiss 75191, Electron Microscope Sciences) covered with adhesive carbon tape. Samples were then sputter-coated with a 2∶1 ratio of gold to palladium for 3 min. Specimens were imaged using either a Zeiss Auriga Crossbeam electron microscope at the University of Tennessee, Knoxville, or a JEOL 6060 electron microscope at the University of Vermont, Burlington. Stubs were initially viewed at low resolution to confirm that there was no contamination. Three spores per stub were then imaged, each at two magnifications: ×5000 and ×15,000. Lower-magnification images were used to assess perine macrostructure, and higher-magnification images were used to assess microstructure on the spore body. Spores were imaged using an accelerating voltage between 5000 and 10,000 kV on both microscopes, adjusted depending on the extent of charging and interference with image quality. Images were adjusted and assembled into plates using Adobe Photoshop CC version 14.2.2.

Character State Coding

Our choice of characters and states was informed by previous studies of perine morphological evolution (Moran et al. 2007, 2010), descriptive studies of fern spore ornamentation (Tryon and Tryon 1982; Tryon and Lugardon 1991), and variation of perine morphology encountered during our sampling. We scored seven perine characters, four of which pertain to macrostructure and three to microstructure. Since we did not use transmission electron microscopy (TEM), we were unable to determine whether macrostructure resulted from perine ornamentation or from the underlying structure of the exine, and we observed only superficial spore morphology. The macrostructure characters were (1) perine adnation to exine, (2) macrostructure folding (broad folds or thin crests), (3) macrostucture form (elongate or echinate), and (4) reticulation (of crests or folds). The microstructure characters were defined as secondary sculpturing (e.g., perforations on a crest), and they were (5) microstructure presence, (6) microstructure type (spiculae, minute crests, minute folds, or verrucae), and (7) perforations. See table 1 for descriptions, character coding, and references to figures representative of character states. In some cases where only low-magnification SEM images were available, the microstructure characters (6, 7) could not be determined and were scored as missing data and notated with a question mark in the matrix (app. S2). In other instances, characters were scored as not applicable and notated with a dash. For example, in taxa with character 5, microstructure presence, scored as absent, character 6, microstructure type, cannot be scored and is thus not applicable.

Character State Reconstructions

Optimizations of the characters on the phylogeny were performed in Mesquite version 3.4 using the Bayesian phylogeny pruned to include only taxa for which spore images were
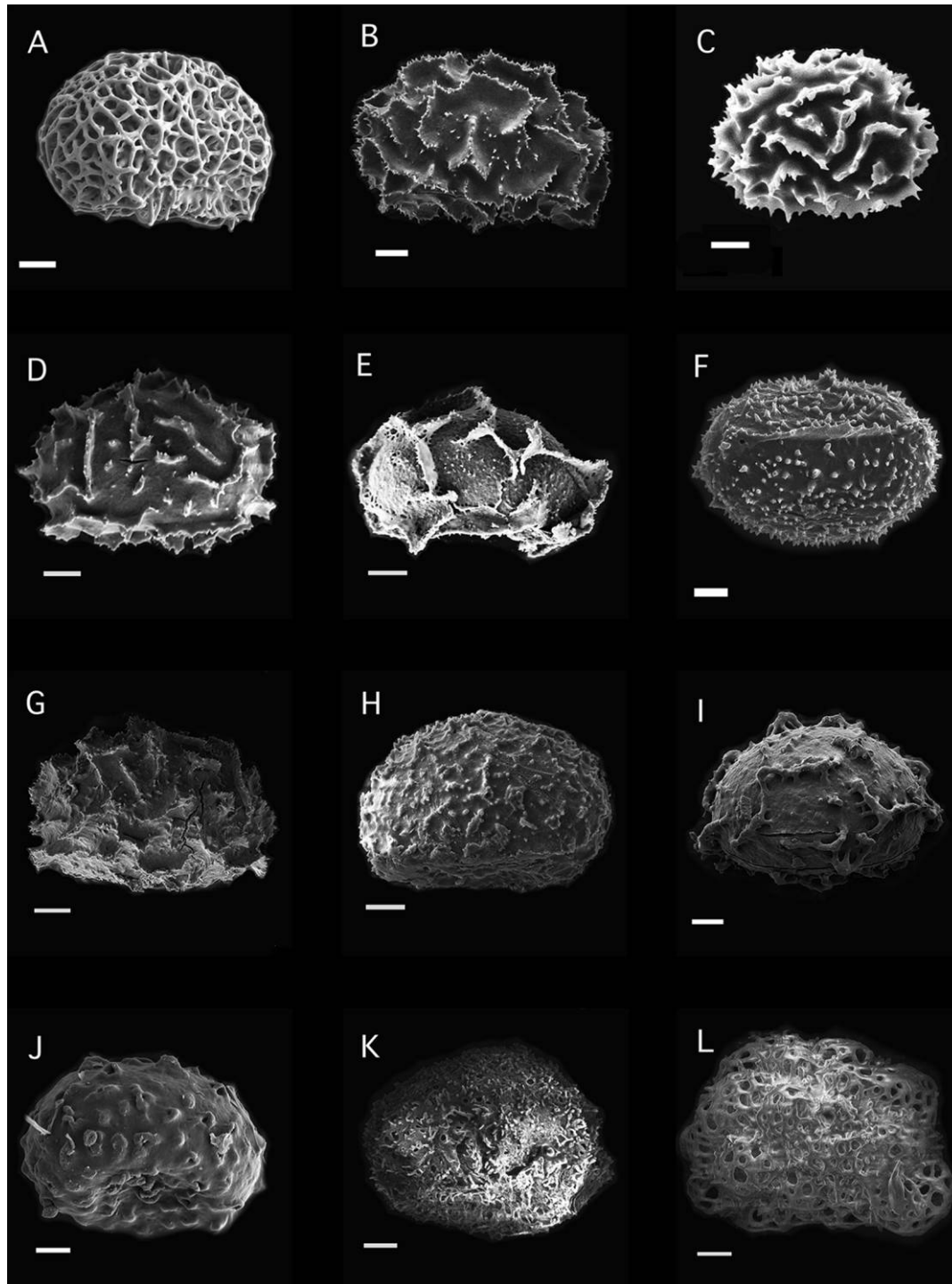
Fig. 1 Representative spores of Thelypteridaceae. *A, Amauropelta* (sect. *Pachyrachis*) *pachyrachis* (Sundue 3298, VT). *B, Amblovenatum opulentum* (Tan 2013103, VT). *C, Chingia fijiensis* (Fawcett 611, VT). *D, Christella* (sect. *Christella*) *acuminata* (Chang 2014002-006, VT). *E, Christella* (sect. *Christella*) *arida* (Hovenkamp 05-23, VT). *F, Christella* (sect. *Christella*) *cyatheoides* (Fawcett 277, VT). *G, Christella* (sect. *Christella*) *harveyi* (Fawcett 629, VT). *H, Christella* (sect. *Christella*) *hispidula* (Pringle s.n., VT). *I, Christella* (sect. *Pelazoneuron*) *normalis* (Zika 7927, VT). *J, Christella* (sect. *Pelazoneuron*) *normalis* (=*Thelypteris kunthii*; Rugg s.n., VT). *K, Christella* (sect. *Pelazoneuron*) *patens* (Grayum 1181, VT). *L, Christella* (sect. *Pelazoneuron*) *tuerckheimii* (Tuerckheim 1200, VT). Scale bars = 5 μm. Taxa named in the following are included in the optimization: *A, B, D, E, H, I, K*.

Table 1

Characters and Their States with Descriptions and Representative Figures

Character	States	Description	Example
1. Perine adnation to exine	(0) Adnate	Smooth or with low verrucae. No macrostructure ornamentation	Not pictured
	(1) Free	Macrostructure ornamentation present, such as thin crests, broad folds, and cones	Figure 3E
2. Macrostructure folding	(0) Broad folds	Folds broader at the base than at the summit	Figure 4L
	(1) Thin crests	Folds of uniform width from base to summit	Figure 5D
3. Macrostructure form	(0) Echinate	Short folds, typically taller than they are long; these may be flattened, cylindrical, or conical	Figure 4H
	(1) Elongate	Elongate folds	Figure 3B
4. Macrostructure reticulation	(0) Not reticulate	Macrostructure that does not interconnect across the surface of the spore	Figure 4H
	(1) Reticulate	Macrostructure that forms a net or reticulum such that it forms multiple enclosed spaces across the spore body	Figure 3D
5. Microstructure	(0) Microstructure absent	A smooth spore body, lacking macrostructure	Figure 2I
	(1) Microstructure present	Finer-scale features on the spore body, featuring small projections such as verrucae or spicules	Figure 3G
6. Microstructure type	(0) Spiculate	Fine microstructure pointed and typically cover most of the spore body	Figure 6A
	(1) Minute Crests	Resembles thin-crest macrostructure but at a finer scale	Figure 6C
	(2) Minute Folds	Resembles broad-fold macrostructure but at a finer scale	Figure 6D
	(3) Verrucae	Small rounded projections across the body	Figure 6B
7. Perforations of perine	(0) Absent	Perine not perforate	Figure 5I
	(1) Present	Perine perforate	Figure 6E

available and scored. Ancestral character state reconstructions were performed under both maximum parsimony (MP) and ML. For MP analysis, states were unordered and equally weighted. The ML optimizations were performed using the MK1 (Markov k-state 1 parameter) model (Lewis et al. 2001) in Mesquite version 3.4. The results of the two analyses were combined into a single figure. Hereafter, likelihood reconstructions for a given node are discussed as having a high likelihood when one state is reconstructed with a proportional likelihood (PL) greater than 0.60. Reconstructions are discussed as ambiguous when all states have a PL less than 0.60.

Tests for Phylogenetic Signal

Phylogenetic signal of each perine character (table 1) was calculated using the pruned BI 50% majority-rule consensus tree, and the retention index (RI) was calculated for the parsimony reconstructions (table A1; tables A1, A2 are available online). We used the function *fitDiscrete* from the package GEIGER (Harmon et al. 2007) implemented in R (ver. 3.4) in order to estimate phylogenetic signal. The log likelihood of each character was calculated for a free model with characters optimized onto a tree with branch lengths derived from the BI consensus tree, as well as with a model where λ is constrained to zero, which sets all branch lengths as equal. A χ^2 test was then used to calculate whether there was a statistically significant difference between the log likelihoods of the two models.

Correlated Character Evolution

Correlations were assessed between perine characters 2–5 and 7 (table 1) using Pagel's (1994) test, as implemented in

Mesquite version 3.4. Likelihood estimation was performed for each pair of characters using default settings, in which a model of independent evolution was compared with a model of correlated evolution. A likelihood ratio test comparing these two models for each pair of characters was performed, and the P value for each comparison was used to assess correlation at a threshold of $P = 0.05$ (table A2). All characters were tested for correlation except characters 1 and 6 because they did not meet the test criteria; character 1 had a sample size of one, while character 6 did not include binary character states. For the other characters, two species, *Phegopteris decursive-pinnata* and *Pronephrium articulatum*, were pruned because of missing data.

Results

Matrix Assembly

Our assembly using SUMAC resulted in a matrix including sequences from three nuclear and eight plastid markers (*atpA*, *atpB*, *LEAFY*, *NEO*, *matK*, *pgiC*, *psbA-trnH*, *rbcL*, *rps4-trnS*, *trnG-trnR*, and *trnL-trnF*), totaling 16,136 base pairs with 203 taxa (available from TreeBase 23496). Assembly of the supermatrix using SUMAC yields an MSDS for each missing sequence (Freyman 2015). This score indicates the extent to which missing data would contribute to the overall decisiveness of the matrix if it were present. Based on our MSDS, there are no outstanding gaps in our data that have a major impact on the decisiveness of the matrix. The addition of *rbcL*, *rps4-trnS*, and *trnL-F* sequences, which are represented across the greatest number of taxa, would contribute most to decisiveness (fig. A1).

Molecular Phylogenetic Analyses

Our molecular phylogeny comprises 11 markers from 203 taxa, representing approximately 20% of the species diversity in the family (fig. A2). Tree topologies generated by BI and ML (not shown) analyses were similar, and both generally had high support along backbone nodes. Nearly all nodes representing the most recent common ancestor (MRCA) of monophyletic genera have posterior probability support values greater than 90. Of the 20 genera represented by more than one species, we recovered 12 as monophyletic (*Cylogramma, Glaphyropteridopsis, Goniopteris, Macrothelypteris, Meniscium, Metathelypteris, Oreopteris, Phegopteris, Pseudophegopteris, Stegnogramma* s.l., *Steiropteris*, and *Thelypteris*) and eight as nonmonophyletic (*Amauropelta, Christella, Coryphopteris, Parathelypteris, Pneumatopteris, Pronephrium, Pseudocyclosorus*, and *Sphaerostephanos*). Within the Thelypteridaceae, there are two monophyletic sister subfamilies: the Phegopteridoideae, which includes the monophyletic genera *Macrothelypteris, Phegopteris*, and *Pseudophegopteris*, and the Thelypteridoideae, which includes all other genera (fig. A2*A*). Within this subfamily, we discuss our results along the backbone of the phylogeny for well-supported monophyletic clades that include the early-diverging Thelypteridoideae, the cyclosoroid clade, and the highly nested christelloid clade.

Among early-diverging Thelypteridoideae (fig. A2*A*), we found strong support for *Thelypteris* s.s., *Oreopteris*, and the ACMP clade (*Amauropelta, Coryphopteris, Metathelypteris*, and *Parathelypteris*; posterior probability [pp] = 100). Within this clade, *Metathelypteris* and the *Coryphopteris* clade (which includes some species currently treated in *Parathelypteris*) are both well supported as monophyletic. The relationships between the mostly Neotropical *Amauropelta* and the East Asian and temperate North American *Parathelypteris* have lower support and are less clear (fig. A2*A*).

The cyclosoroid genera *Cyclogramma, Goniopteris, Meniscium, Stegnogramma*, and *Steiropteris* are each monophyletic and well supported (fig. A2*B*). *Ampelopteris, Mesophlebion*, and *Cyclosorus* s.s. are each represented by a single taxon and together form a well-supported clade.

Nested within the cyclosoroids, the christelloid clade is well supported, although many of the genera within it are not (fig. A2*C*). *Pneumatopteris* is polyphyletic, with each of the three species resolved in different places in the phylogeny. The 12 species of *Pronephrium* are resolved in five places. *Pronephrium articulatum* is nested within *Pseudocyclosorus*, rendering the latter nonmonophyletic, and three species are in a clade sister to *Sphaerostephanos elatus*. Five species are in a monophyletic clade that forms a polytomy with *Mesopteris tonkinensis* and a christelloid core group of 48 species, and three other species form a clade with *Chingia longissima* nested within it. Six species of *Sphaerostephanos* form a clade (pp = 88), while *Sphaerostephanos unitus* is sister to a clade of eight other christelloid genera, and *S. elatus* is sister to a clade of three *Pronephrium* species. The genus *Christella* resolves as two distinct clades, with one corresponding to the predominantly Asian, well-supported *Christella* sect. *Christella* clade and the other to the African and American *Christella* sect. *Pelazoneuron*. The genera *Amblovenatum, Chingia, Mesopteris, Nannothelypteris, Plesioneuron*, and *Trigonospora* are

each represented by a single accession, while the two species of *Glaphyropteridopsis* are well supported as a clade.

Perine Morphological Characters

Character optimizations for characters 2–7 are depicted on the pruned phylogenies, with MP and ML results combined (TreeBase 23495). The 16 backbone nodes are numbered to facilitate presentation of the results (fig. 7). A synopsis of the perine morphology for each genus (excluding *Menisorus* and *Nannothelypteris*) synthesizing our results with previous findings is provided.

Macrostructure adnation. Appressed (adnate) perine is autapomorphic for *Phegopteris decursive-pinnata*; all other spores have a loosely attached (free) perine. The reconstruction is unambiguous and therefore not shown.

Macrostructure folding. For most species sampled, the macrostructure has broad folds (e.g., figs. 1*I*, 2*I*), with thin crests less common (e.g., figs. 1*B*, 1*E*, 2*C*). The ML reconstruction indicates with high likelihood (PL > 0.6) that 14 of 16 backbone nodes have broad folds (fig. 7*A*). The reconstructed state is ambiguous for nodes 5 and 6.

Broad folds are ancestral for the Phegopteridoideae (PL = 0.8), and among species with macrostructure present, all spores have broad folds. Three clades within Thelypteridoideae, ACMP, *Thelypteris*, and *Oreopteris*, feature three transitions to thin crests and three reversals to broad folds. The MRCA of the ACMP clade is reconstructed as broad folds with high likelihood (PL = 0.7). For the ancestor of the cyclosoroids, broad folds are reconstructed as ambiguous (nodes 5 and 6) with several gains and losses. In the nonchristelloid cyclosoroids, there are four or five transitions to the alternate state, with two subsequent reversals to broad folds. Broad folds are reconstructed as ancestral in the christelloid clade as well (node 9; PL = 0.99), with seven independent transitions to thin crests. Four of these transitions occur within the genus *Christella* (fig. 7*A*).

Among taxonomic groups, thin crests characterize all taxa sampled in *Pronephrium* sect. *Grypothrix* (*Pronephrium cuspidatum, Pronephrium simplex, Pronephrium triphyllum*; fig. 4*I*–4*K*) and *Steiropteris* (fig. 5*J*). Broad folds that are short and echinate characterize *Pseudocyclosorus* (fig. 5*E*). In the ancestral character reconstruction, broad folds characterize all sampled taxa in *Glaphyropteridopsis* (fig. 2*G*), *Metathelypteris* (fig. 3*I*–3*L*), *Pseudophegopteris* (fig. 5*F*), and *Stegnogramma* (fig. 5*I*).

Macrostructure form. Elongate folds or crests (e.g., figs. 1*D*, 3*E*) are reconstructed with high likelihood (PL > 0.6) as the ancestral character state along all backbone nodes (fig. 7*A*). Within the Phegopteridoideae, there is one transition to echinate macrostructure. Within the Thelypteridoideae, echinate macrostructure evolves in *Thelypteris* s.s. and *Oreopteris quelpaertensis* and several times within the cyclosoroids with reversals (fig. 7*A*). The Thelypteridoideae group comprising ACMP, *Thelypteris*, and *Oreopteris* includes two transitions to echinate macrostructure (e.g., fig. 4*F*–4*H*). The MRCA of the ACMP clade is unambiguously reconstructed as elongate (PL = 1), and all members of the clade feature elongate macrostructure. Reconstruction suggests that the MRCA of the cyclosoroids
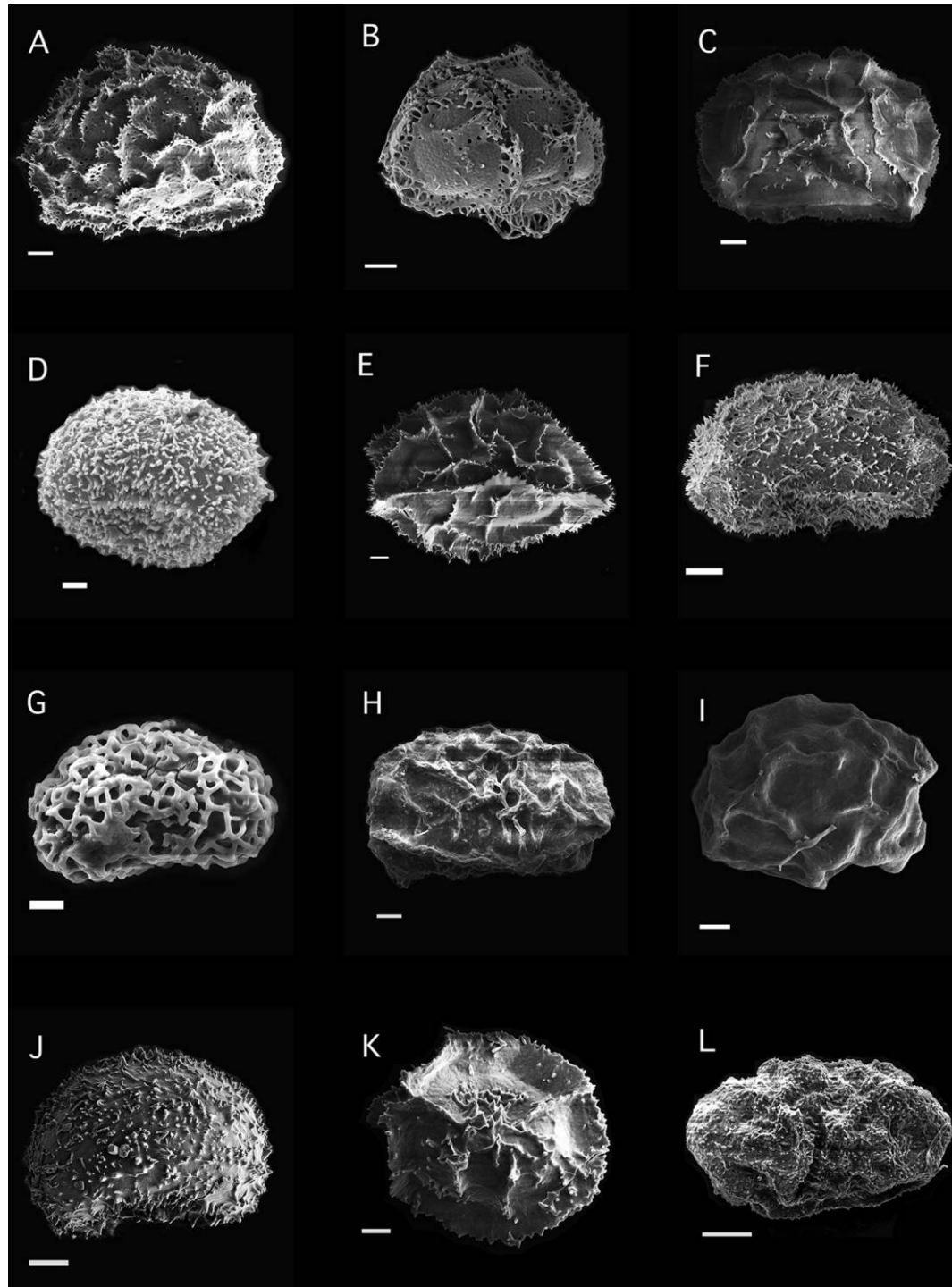
Fig. 2 Representative spores of Thelypteridaceae. *A, Parathelypteris* (*Coryphopteris*) *simulata* (Fawcett 593, VT). *B, Coryphopteris japonica* (Chang 20080423, VT). *C, Coryphopteris japonica* (Ming 844, VT). *D, Coryphopteris obtusata* (Karger 1174, VT). *E, Cyclogramma auriculata* Jinn-Fen (Chen s.n., VT). *F, Cyclosorus interruptus* (Given 11096, VT). *G, Glaphyropteridopsis rufostraminea* (Zhang 20100618027, VT). *H, Goniopteris abdita* (Fawcett 457, VT). *I, Goniopteris* aff. *verecunda* (Fawcett 423, VT). *J, Goniopteris cordata* (Fawcett 454, VT). *K, Goniopteris hastata* (Fawcett 374, VT). *L, Goniopteris hildae* (Fawcett 369, VT). Scale bars = 5 μm. Taxa named in the following are included in the optimization: *A–C, E–H, J, L*.
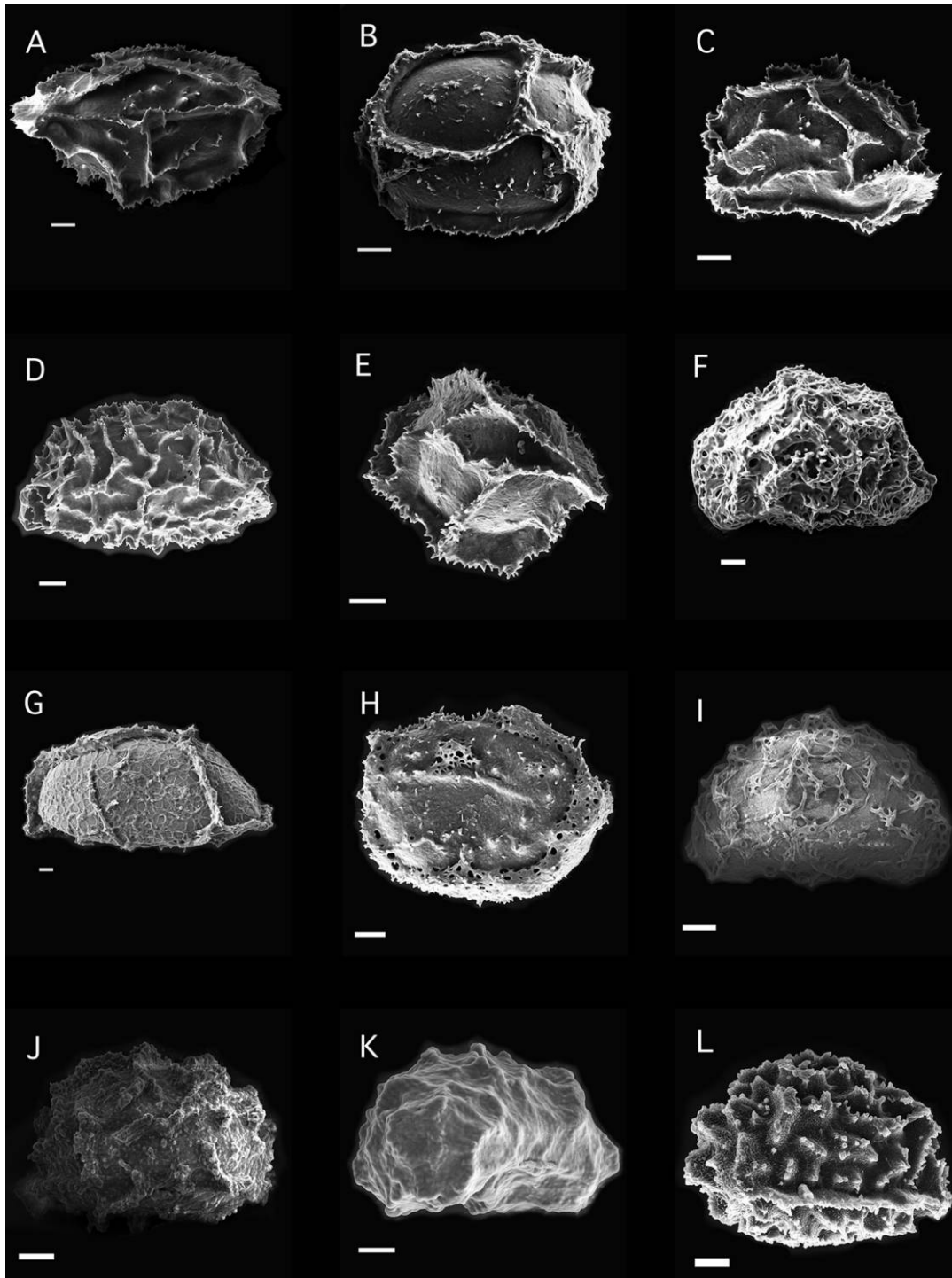
Fig. 3 Representative spores of Thelypteridaceae. *A, Goniopteris moranii* (Fawcett 437, VT). *B, Goniopteris paranaensis* (Labiak 3624, VT). *C, Goniopteris pennata* (Conant 1561, VT). *D, Goniopteris tetragona* (Duss 856, VT). *E, Goniopteris vivipara* (Haerchen 104, VT). *F, Macrothelypteris torresiana* (Fawcett 696, VT). *G, Meniscium lanceum* (Sundue 890, VT). *H, Meniscium longifolium* (Conant 895, VT). *I, Metathelypteris adscendens* (Pi-Fong Lu 22878, VT). *J, Metathelypteris* sp. (Chiou15262, VT). *K, Metathelypteris gracilescens* (Elmer 11485, VT). *L, Metathelypteris uraiensis* (Pi-Fong Lu 9197, VT). Scale bars = 5 μm. Taxa named in the following are included in the optimization: *A, C–F, H, K, L*.
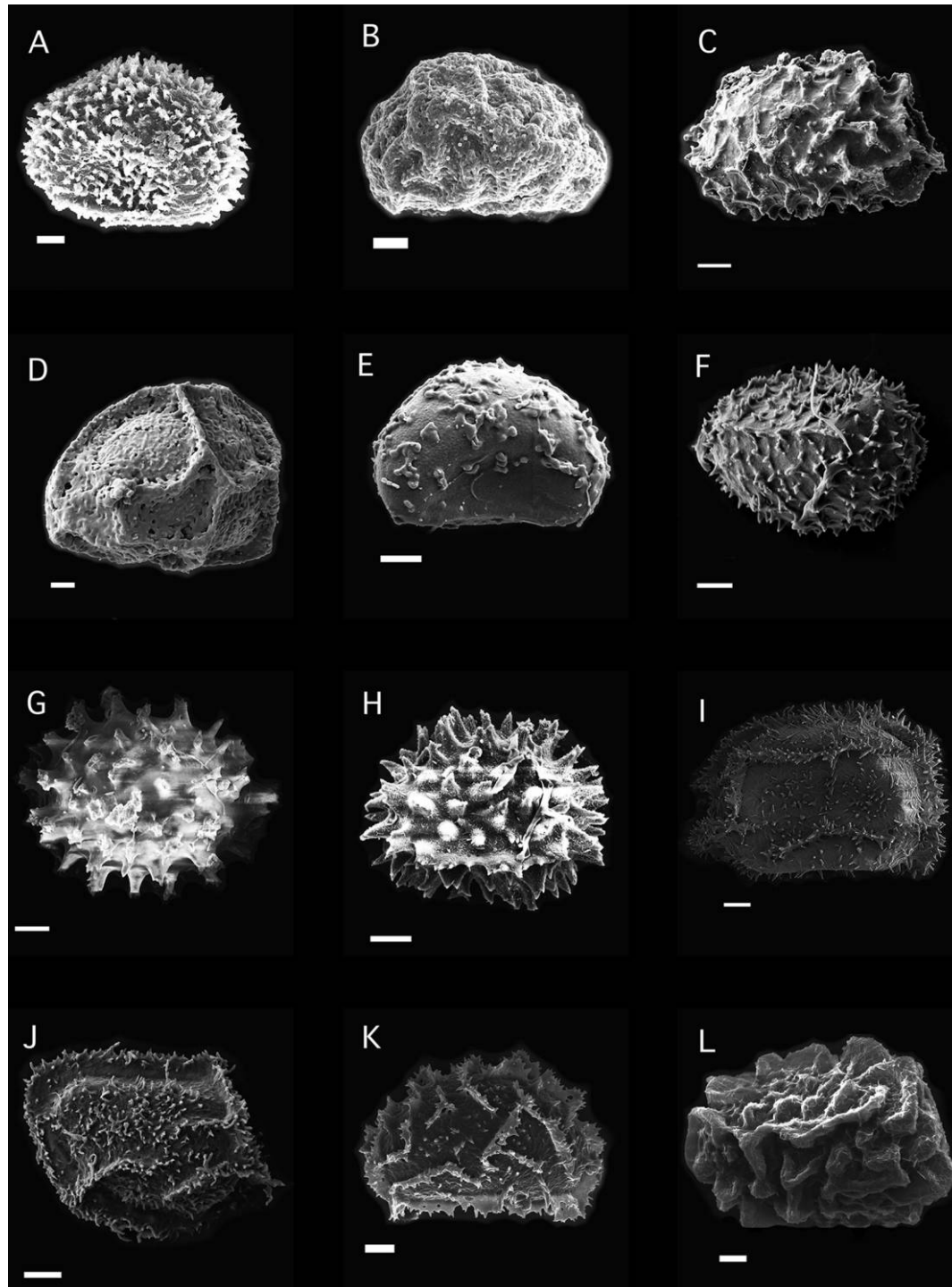
Fig. 4 Representative spores of Thelypteridaceae. *A, Oreopteris quelpaertensis* (Barrington 2408, VT). *B, Parathelypteris beddomei* (Sundue 1726, VT). *C, Parathelypteris nevadensis* (Fawcett 821, VT). *D, Phegopteris connectilis* (Patel 66, VT). *E, Phegopteris hexagonoptera* (Patel 90, VT). *F, Pneumatopteris* aff. *microloncha* (Wade 3995-2, VT). *G, Pneumatopteris* cf. *sogerensis* (Elmer 98845, VT). *H, Pneumatopteris sogerensis* (Karger 1067, VT). *I, Pronephrium* (sect. *Grypothrix*) *cuspidatum* (Pi-Fong Lu 11090, VT). *J, Pronephrium* (sect. *Grypothrix*) *simplex* (Pi-Fong Lu 9270, VT). *K, Pronephrium* (sect. *Grypothrix*) *triphyllum* (Sundue 2243, VT). *L, Pronephrium* (sect. *Menisciopsis*) *penangianum* (Ming 2846, VT). Scale bars = 5 μm. Taxa named in the following are included in the optimization: *A–E, I–L*.
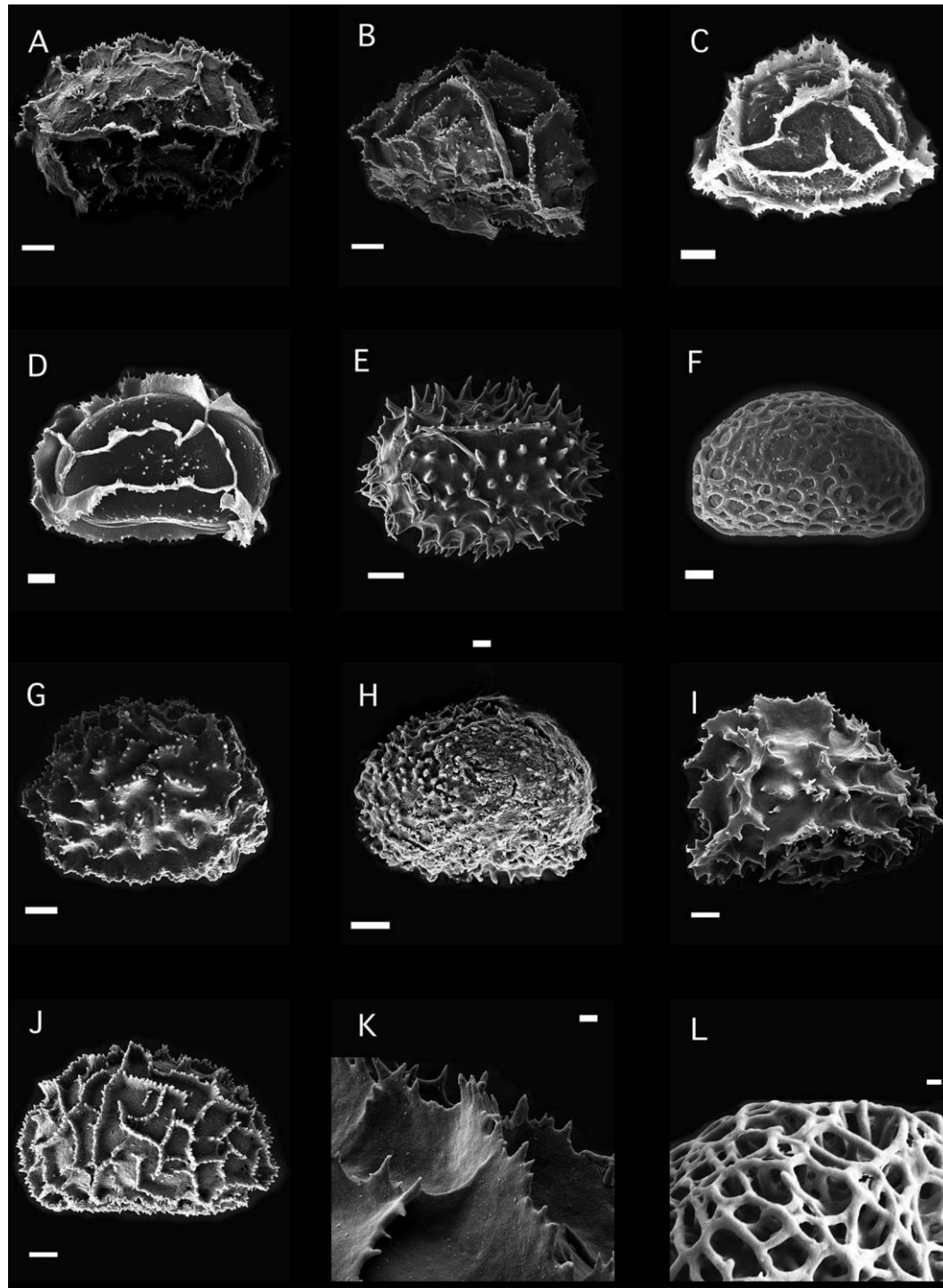
1024

Fig. 5 Representative spores of Thelypteridaceae. *A*, *Pronephrium* (sect. *Pronephrium*) *asperum* (James and Sundue 1693, VT). *B*, *Pronephrium* (sect. *Pronephrium*) *asperum* (Elmer 10972, VT). *C*, *Pronephrium* (sect. *Pronephrium*) *peltatum* (Hovenkamp 05-256, VT). *D*, *Pronephrium* (sect. *Pronephrium*) *womersleyi* (Sundue 3726, VT). *E*, *Pseudocyclosorus esquirolii* (Pi-Fong Lu 24229, VT). *F*, *Pseudophegopteris aurita* (Sundue 3799, VT). *G*, *Sphaerostephanos polycarpus* (Tan 2011170, VT). *H*, *Sphaerostephanus unitus* (Fawcett 614, VT). *I*, *Stegnogramma pozoi* (Boufford 20072, VT). *J*, *Steiropteris glandulosa* (Hill 28047, VT). *K*, *Cyclogramma auriculata* (Jinn-Fen Chen s.n., VT). *L*, *Amauropelta pachyrachis* (Sundue 3298, VT). Scale bars = 5 μm (*A–J*), 1 μm (*K*, *L*). Taxa named in the following are included in the optimization: *A*, *B*, *E–H*, *J–L*.
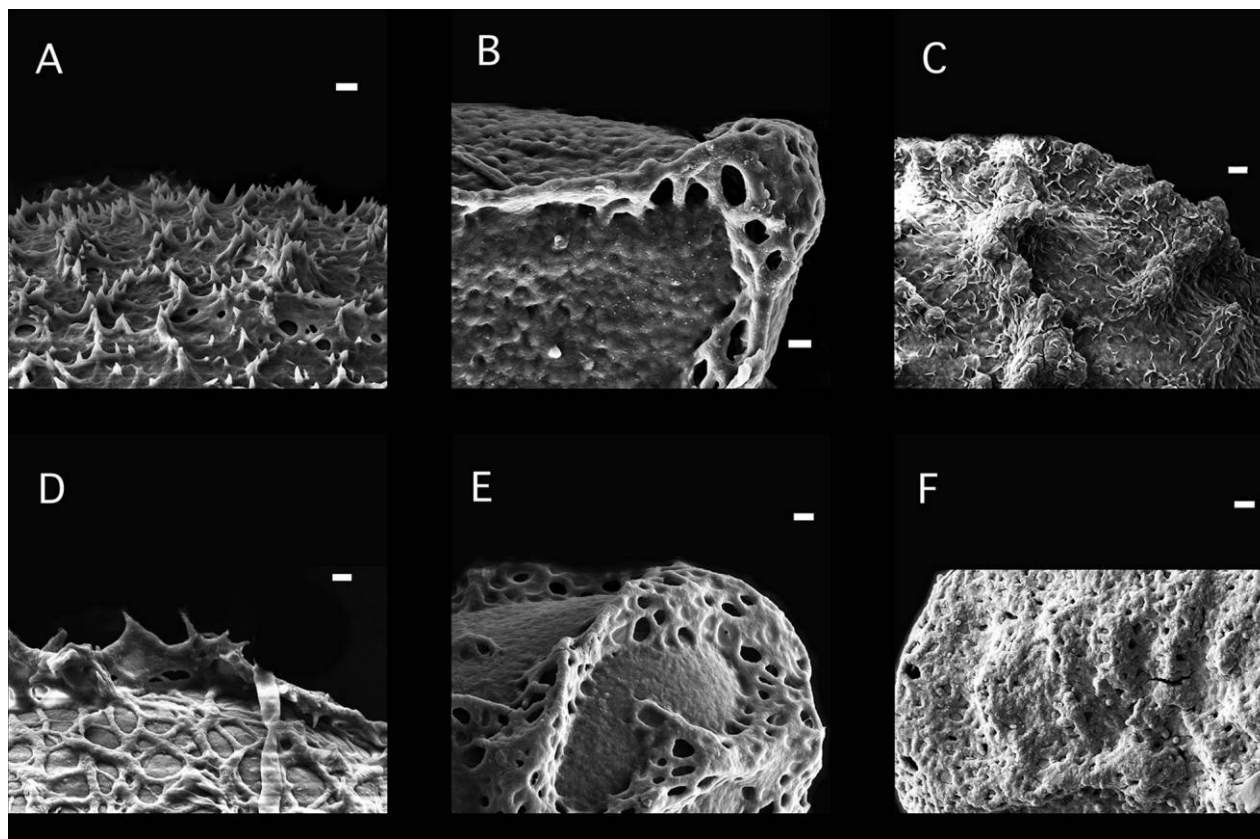
1025

Fig. 6   Spore microstructure details of Thelypteridaceae. *A, Cyclosorus interruptus* (Given 11096, VT). *B, Parathelypteris angustifrons* (Charette 1522, VT). *C, Pneumatopteris costata* (Fawcett 646, VT). *D, Meniscium lanceum* (Sundue 890, VT). *E, Metathelypteris laxa* (Charette 1472, VT). *F, Parathelypteris beddomei* (Sundue 1726, VT). Scale bars = 1 μm. Taxa named in the following are included in the optimization: *A, B, E, F.*

features elongate macrostructure (node 5; PL = 0.91), and the nonchristelloid cyclosoroids feature three or four transitions to echinate macrostructure, with two or three subsequent reversals to the ancestral elongate macrostructure (fig. 7*A*). The christelloid group includes nine transitions to echinate macrostructure, with three subsequent reversals to the ancestral elongate macrostructure. Four of the nine transitions to echinate macrostructure in the christelloids are reconstructed as autapomorphies within *Christella*.

In the ancestral character reconstruction, all sampled taxa in *Thelypteris* and *Stegnogramma* feature short, echinate macrostructure (fig. 7*A*). *Stegnogramma* features a unique exception not included in the reconstruction. All but one species of sister genus *Cyclogramma* also feature short, echinate macrostructure. *Pronephrium nudatum* and *P. triphyllum*, which are resolved in separate sections of *Pronephrium*, appear to have evolved echinate macrostructure convergently. Elongate macrostructure characterizes *Glaphyropteridopsis, Goniopteris, Macrothelypteris, Metathelypteris, Pseudophegopteris, Steiropteris*, and the ACMP clade. For these genera, elongate macrostructure is also reconstructed as the ancestral state (PL = 1).

Reticulation.   Reticulate macrostructure (e.g., figs. 1*A*, 5*F*) is reconstructed as ancestral with high likelihood (PL > 0.6) at 9 of the 16 backbone nodes; the PL for the reticulate state

is greatest among early-diverging lineages and transitions gradually to nonreticulate among the more recently diverged lineages; within christelloids (nodes 12–16), the ancestral states are strongly nonreticulate (fig. 7*A*).

The MRCA for the Phegopteridoideae, which is also the MRCA for the Thelypteridaceae, is reconstructed as reticulate (fig. 7*A*; node 1; PL = 0.9). The Phegopteridoideae includes one transition to nonreticulate macrostructure. The Thelypteridoideae group comprising ACMP, *Thelypteris*, and *Oreopteris* includes three transitions to nonreticulate macrostructure and two subsequent reversals to the ancestral reticulate macrostructure. The MRCA of the ACMP clade is reconstructed as reticulate with a high likelihood (PL = 0.82). The MRCA of the cyclosoroids also features reticulate macrostructure in our reconstruction (node 5; PL = 0.88), and the nonchristelloid cyclosoroids include two transitions to nonreticulate macrostructure with two reversals to reticulate macrostructure (fig. 7*A*). The ancestral state for the christelloids clade is ambiguous (node 9), and the group features six to eight transitions to the alternate character state (fig. 7*A*).

Reticulate macrostructure is characteristic of *Glaphyropteridopsis, Goniopteris, Macrothelypteris, Pseudophegopteris*, and *Steiropteris*. Nonreticulate macrostructure is characteristic of taxa sampled in *Pseudocyclosorus, Stegnogramma*, and

Thelypteris. Both states are found in the genera *Cyclogramma*, *Christella* sect. *Pelazoneuron*, *Christella* sect. *Christella*, *Metathelypteris*, *Oreopteris*, and *Phegopteris*.

Microstructure.   Microstructure (fig. 6) is unambiguously reconstructed as present with high likelihood (PL > 0.6) at eight of 16 backbone nodes, all within the christelloid clade (fig. 7B). The character state reconstructions at the remaining backbone nodes are ambiguous. Taxa in the Phegopteridoideae largely feature perine without microstructure; however, the ancestral state for the group is ambiguous (node 1), and the clade includes two or three transitions and one or two reversals (fig. 7B). The MRCA of the ACMP clade is reconstructed with high likelihood as microstructure present (PL = 0.66). The ancestral state for the MRCA of the cyclosoroids is also ambiguous (node 5), with four or five transitions and two or three subsequent reversals (fig. 7B). The MRCA of the christelloids is reconstructed as microstructure present (node 9; PL = 0.71), and the group features eight transitions to microstructure absent with three or four subsequent reversals to microstructure present (fig. 7B).

The absence of microstructure is characteristic of all taxa sampled in the genera *Pseudophegopteris* and *Stegnogramma*. Presence of microstructure is characteristic of all sampled taxa in *Meniscium*.

Microstructure type.   Reconstructions of character states pertaining to microstructure type (e.g., fig. 6) are highly variable across the phylogeny, with few discernable patterns. Nonetheless, spiculate microstructure is reconstructed as ancestral at 12 of 16 backbone nodes with high likelihood. Excluding inapplicable data, within the cyclosoroids, there are four transitions to minute crests (fig. 7B).

No single microstructure state is characteristic of all taxa in any genus. However, spiculate microstructure is reconstructed with high likelihood as ancestral for the genera *Goniopteris* and *Meniscium*.

Perforations.   Perforations (e.g., fig. 6E) are reconstructed as absent at all 16 backbone nodes with high likelihood and are absent from most genera in Thelypteridaceae (fig. 7B). Within the Phegopteridoideae, perforations are synapomorphic for *Macrothelypteris*, with a single reversal. Perforations are also synapomorphic for the ACMP clade, with separate reversals in three species. The four backbone nodes within the nonchristelloid cyclosoroids are unambiguously reconstructed as perforations absent, and accordingly, the MRCA of the group is reconstructed as perforations absent (node 5; PL = 1). The group includes two transitions to perforations present and two subsequent reversals to perforations absent in the *Meniscium* clade (fig. 7B). The eight backbone nodes within the christelloids are reconstructed with high likelihood as perforations absent, including the MRCA of the group (node 9; PL = 0.99). The group includes four or five transitions to perforations present and one subsequent reversal to perforations absent in the genus *Christella* (fig. 7B).

The presence of perforations is not characteristic of all taxa sampled for any monophyletic genus. The absence of perforations is featured in all sampled taxa for *Cyclogramma*, *Glaphyropteridopsis*, *Goniopteris*, *Oreopteris*, *Pseudocyclosorus*, *Pseudophegopteris*, *Stegnogramma*, *Steiropteris*, and *Thelypteris*. Also, perforations are present in most of the ACMP clade, with only three exceptions. Perforations absent is the ancestral state for all genera except those within the ACMP clade, as well as *Macrothelypteris* (fig. 7B).

Phylogenetic Signal, Homoplasy, and Correlated Evolution

Character 1, perine adnation, is autapomorphic and not discussed further. For all other characters, phylogenetic signal was significant (table A1). The character reticulation has the strongest phylogenetic signal ($\lambda = 0.972$, $P = 1.011$ e^{-15}), followed by the character microstructure ($\lambda = 0.948$, $P = 5.064$ e^{-13}). The characters microstructure type ($\lambda = 0.922$, $P = 3.893$ e^{-5}) and macrostructure folding had similar values ($\lambda = 0.921$, $P = 1.005$ e^{-5}). The highest RI value is associated with the character reticulation (RI = 0.714), and the RI values were greater than 0.5 for all characters except microstructure type and macrostructure folding.

As expected, there is some relationship between RI values and phylogenetic signal. Reticulation, the character with the strongest phylogenetic signal, also has the highest RI. In addition, the characters with RI values lower than 0.5, macrostructure folding and microstructure type, are also the two characters with weaker phylogenetic signal than the other characters (table A1).

We found that the character macrostructure form is significantly correlated with the characters macrostructure folding, reticulation, microstructure, and perforations (table A2). The character macrostructure folding is also correlated with the character reticulation.

Synopsis of Perine Morphology for Thelypteridaceae Genera

Here, we provide a synopsis of perine morphology for each genus based on a synthesis of our own findings and previous publications. The reported percent of species sampled refers to the number of taxa in our character optimization, but the discussion incorporates previous findings. The genera recognized follow the Pteridophyte Phylogeny Group (PPG I 2016), and any infrageneric classification follows Holttum (1971, 1974, 1982).

Amauropelta Kunze.   Seven of 215 species (3%) sampled (figs. 1A, 5L). Our samples represent four of the nine sections recognized by Smith (1974). Perine morphology among the sampled species is similar, scored as broad folds that are reticulate and perforate (perforations are present in all taxa except *A. oppositiformis*; fig. 1A). In this study, all three states are reconstructed as ancestral for the genus (PL = 0.99, 1, 0.98). These features are consistent with those described by previous authors (Wood 1973; Tryon and Lugardon 1991; Alvarez-Fuentes 2010). In this study, all three states act as synapomorphies for the ACMP clade. However, some homoplasy does exist. A similar finely reticulate perine morphology is also present in the distantly related genus *Macrothelypteris* (fig. 3F; Wood 1973), and a similar but generally coarser reticulum occurs in *Phegopteris* (fig. 4D, 4E) and also in the distantly related genus *Glaphyropteridopsis*.

Amblovenatum J.P.Roux.   One of 12 species (8%) sampled (fig. 1B). *Amblovenatum opulentum* has spores with elongate, thin crests. It also features minute crests.
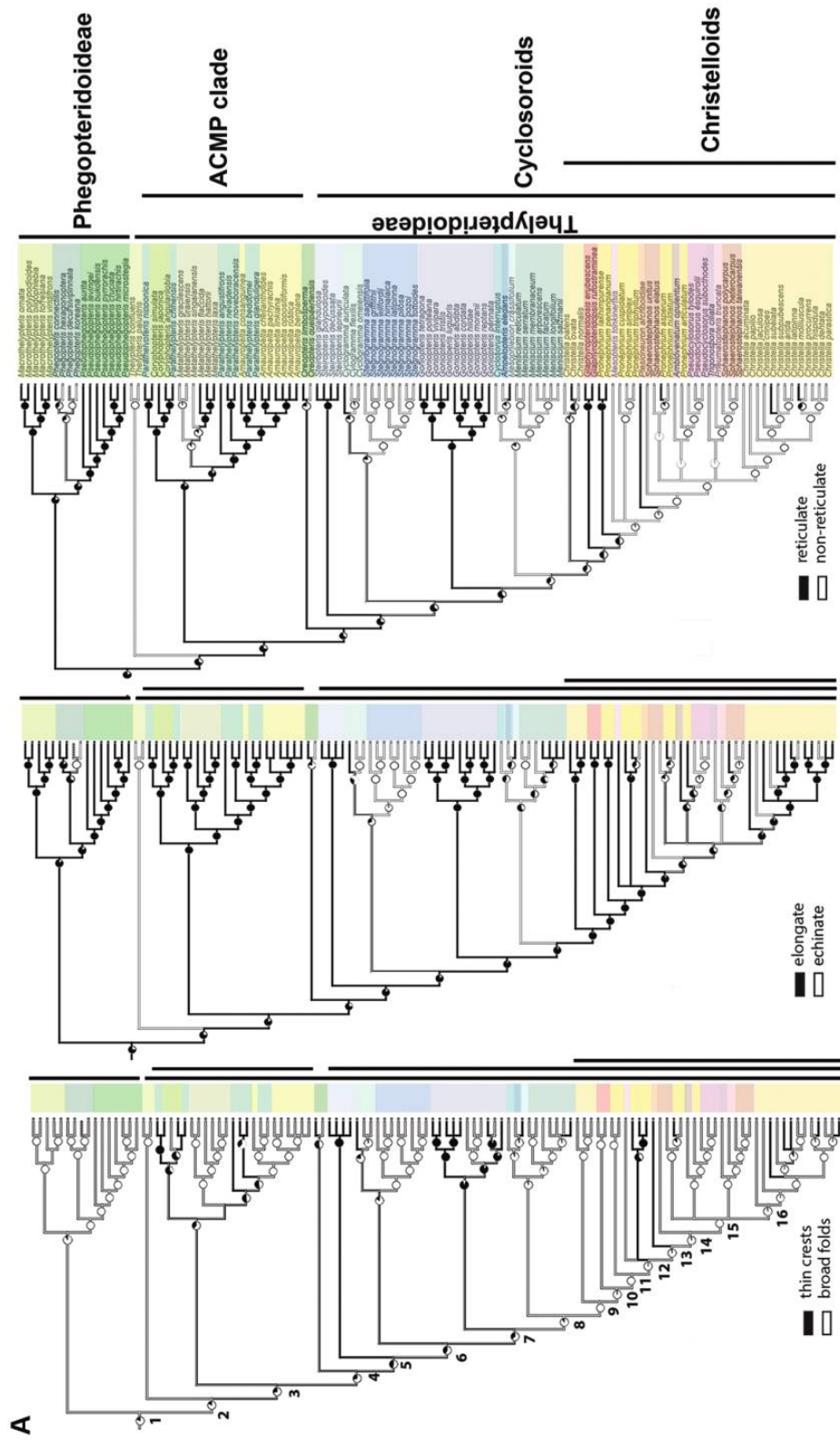
Fig. 7 Optimization of perine characters 2–4 (*A*) and perine characters 5–7 (*B*) onto a pruned 50% majority-rule consensus tree generated from Bayesian inference of 118 Thelypteridaceae species. Parsimony ancestral character reconstruction is indicated by the coloration on the branches, and the likelihood optimizations are shown as pie charts representing proportional likelihood values for each character state. Legends indicate the colors associated with each character state. Character 6, microstructure type, includes additional coloration to indicate ambiguous likelihood reconstruction for a given node as a result of missing or nonapplicable data.
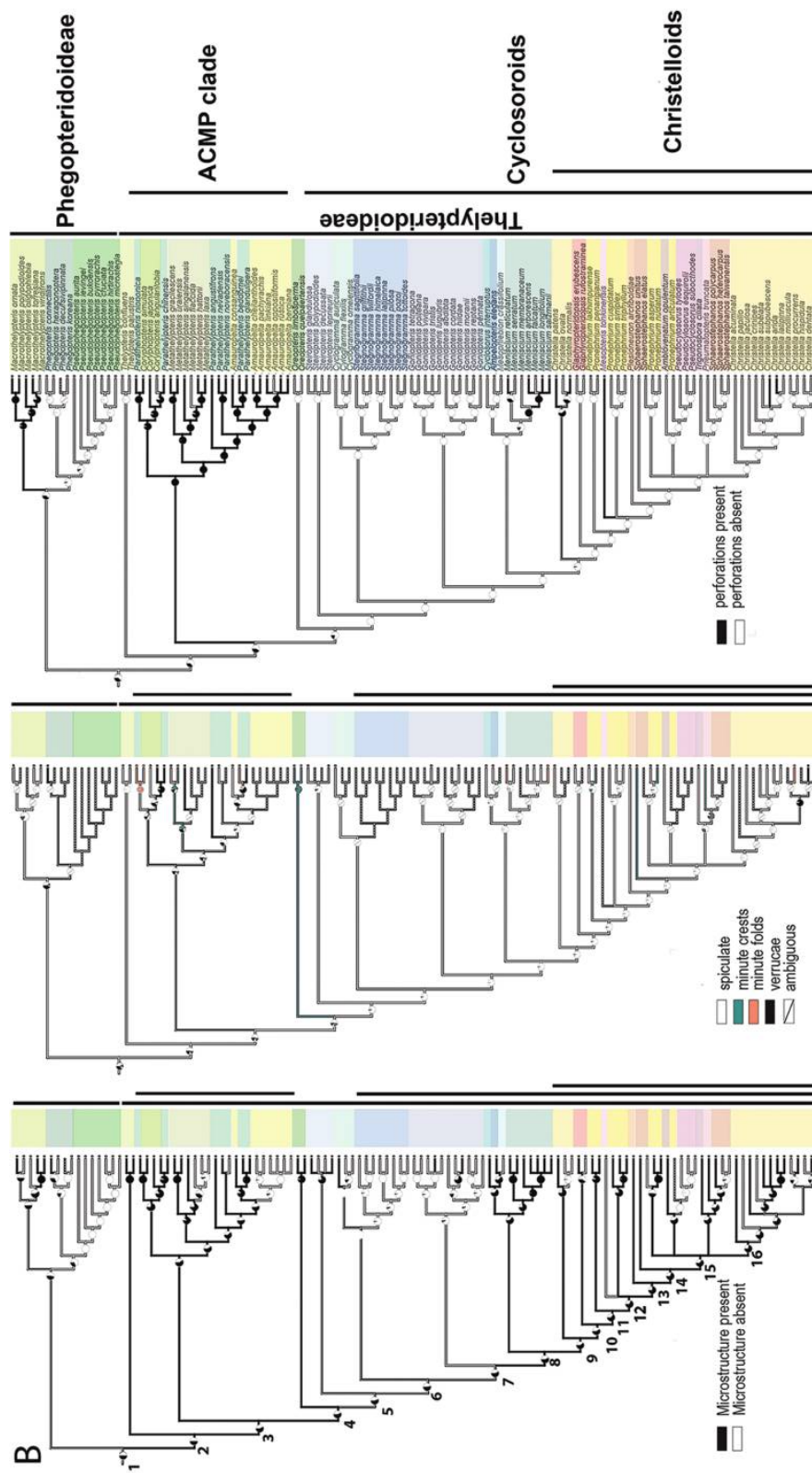
Fig. 7 (*continued*)

Ampelopteris prolifera Kunze. The single species (100%) is sampled. The spores of this species feature broad folds with spiculate microstructure.

Christella Lév. Sixteen of 70 species (23%) sampled (fig. 1*D*– 1*L*). The two subgenera are each monophyletic, while the genus is not. Thirteen species in our optimization correspond to *Christella* sect. *Christella* and three to *Christella* sect. *Pelazoneuron* (Holttum 1974). Even when these two clades are accounted for, *Christella* shows extraordinary variability in perine morphology, exhibiting thin crests or broad folds, as well as reticulate and nonreticulate macrostructure and minute folds, minute crests, or verrucae for microstructure type. Our results corroborate Smith (1971), Tryon and Lugardon (1991), and Dai et al. (2002).

Coryphopteris Holttum. Five of 47 species (11%) sampled (fig. 2*A*–2*D*). The *Coryphopteris* clade is sister to the other genera in the ACMP clade and includes some species most commonly treated as *Parathelypteris* sensu Ching (fig. A2). All taxa sampled in *Coryphopteris* have elongate, reticulate macrostructure and feature some type of microstructure. However, they vary in microstructure type and presence of perforations. Our specimen of *C. japonica* from Jiangxi, China, has thin crests, but the spores of our specimen from Taiwan have broad folds. Nakato et al. (2004) demonstrated extraordinary variability of perine morphology that corresponds to ploidy within the *C. japonica* complex, with spores exhibiting perines that were echinate (diploid), had broad folds (triploid), or had thin crests (tetraploid); all specimens in their study were from Japan or Korea. The North American species *Parathelypteris simulata* is recovered as a member of the *Coryphopteris* clade and is now treated in that genus (Fawcett 2018).

Cyclogramma Tagawa. Three of eight species (38%) sampled (figs. 2*E*, 5*K*). Broad folds that are conical and nonreticulate (echinate) are ancestral for the genus (PL = 0.77, 0.68, 0.75) and shared by its sister genus *Stegnogramma* (Wood 1973; Zhang 1990). *Cyclogramma auriculata*, the type of the genus, has spores with thin, elongate crests that are reticulate (fig. 2*E*).

Cyclosorus Link. One of two species (50%) sampled (fig. 6*A*). *Cyclosorus interruptus* is pantropical, and its geographical variants warrant further study. The perine of our New Zealand specimen of *C. interruptus* exhibits spiculate microstructure and echinate macrostructure (fig. 2*F*) and resembles the image of the Panamanian specimen in Tryon and Lugardon (1991). Both of these differ from the Chinese specimen in Wang and Dai (2010), which has crests.

Glaphyropteridopsis Ching. Two of four species (50%) sampled (fig. 2*G*). The species sampled have reticulate, elongate, broad folds, and all three states are ancestral for the genus (PL = 1, 0.99, 0.99). The two sampled species have different microstructure.

Goniopteris C. Presl. Eleven of the 120 species (9%) sampled (figs. 2*H*–2*L*, 3*A*–3*E*). Perine macrostructure is largely characterized by elongate, reticulate, thin crests, which are states ancestral for the genus (PL = 0.997, 1). An exception to thin crests may be seen in four Antillean calciphiles, *G. reptans*, *G. abdita*, *G. hildae*, and *G. verecunda*, which have broad folds. All species lack microstructure (character 5; fig. 5*I*) except *G. hildae*. Our sample of *G. cordata* (S. Fawcett 454) includes a mixture of well-developed and apparently abnormally developed spores; our image (fig. 2*J*) depicts the irregular form. All other observations indicate that other spores have the typical reticulate macrostructure of the genus.

Macrothelypteris (H. Itô) Ching. Five of ten species (50%) sampled (fig. 3*F*). Elongate, broad, reticulate folds characterize the genus based on our sample. Perforate, elongate, broad folds and reticulation are ancestral states for the clade (PL = 0.999, 1, 1, 0.99). Perforate spores distinguish *Macrothelypteris* from all other members of the Phegopteridoideae, although perforate spores are absent in *M. viridifrons*. Microstructure is highly variable in the group. As noted by Wood (1973), the perforations closely resemble those of *Amauropelta*, though the genus is not closely related to *Macrothelypteris*.

Meniscium Schreber. Seven of 27 species (26%) sampled (figs. 3*G*, 3*H*, 6*D*). Perine morphology in *Meniscium* is surprisingly diverse in contrast to the relatively uniform sporophytes. *Meniscium falcatum*, *M. longifolium*, *M. salzmanii*, and *M. arborescens* constitute a monophyletic group within *Meniscium* (fig. A2*B*), and elongate perine morphology is a feature of all of these taxa, whereas the remaining species in the genus are characterized by echinate macrostructure. The only trait diagnostic for this genus in our sampling is the character reticulation, with nonreticulate macrostructure being ancestral for the group (PL = 1). The varied morphology of the genus can be seen in Fernandes et al. (2014).

Mesophlebion Holttum. One of 15 species (7%) sampled. Spores of *M. crassifolium* have elongate, thin crests that are reticulate. Microstructure and perforations are absent.

Mesopteris Ching. The single species (100%) is sampled. *Mesopteris tonkinensis* (C.Chr.) Ching has spores featuring elongate, broad folds that are reticulate (Wang and Dai 2010); however, the image in Wang et al. (2015) is neither perforate nor reticulate.

Metathelypteris (H.Ito) Ching. Six of 12 species (50%) sampled (figs. 3*I*–3*L*, 6*E*). All sampled species of *Metathelypteris* feature broad folds that are elongate, characters that are ancestral for the clade (PL = 0.9801, 0.9970). *Metathelypteris flaccida*, *M. hattorii*, and *M. laxa* form a clade within the genus, and members of this clade are reticulate and lack microstructure, while *M. singalanensis*, *M. uraiensis*, and *M. gracilescens* all feature nonreticulate macrostructure and feature microstructure. Only one species, *M. flaccida*, features perforations.

Oreopteris Holub. Two of three species (67%) sampled (fig. 4*A*). The two species sampled have strikingly different perine morphologies, as recognized by Wood (1973) and Tryon and Lugardon (1991). *Oreopteris quelpaertensis* exhibits broad folds, while *O. limbosperma* has thin crests (fig. 7*A*). The ancestral state for the clade is reconstructed as broad folds (PL =0.87). *Oreopteris quelpaertensis* also features conical macrostructure, while *O. limbosperma* features elongate macrostructure. Echinate macrostructure is reconstructed as ancestral for *Oreopteris* (PL = 0.77). Both sampled species feature microstructure of minute crests, as well as perforations.

Parathelypteris (H.Ito) Ching s.s. Five of 15 species (33%) sampled (figs. 4*B*, 4*C*, 6*B*, 6*F*). *Parathelypteris* is not monophyletic, with some species retained for now in *Parathelypteris* s.s. and others in *Coryphopteris*. Furthermore, we were unable to find characters that are synapomorphic for either of these clades. Holttum (1971), whose spore observations were primarily limited to light microscopy, noted that species

of *Parathelypteris* have rather opaque spores, while in *Coryphopteris* the spores are somewhat translucent.

Phegopteris (C.Presl) Fée. Four of six species (67%) sampled (fig. 4*D*, 4*E*). Perine morphology is variable in the genus. *Phegopteris decursive-pinnata* is the only species with an adnate perine, a trait unique in the family (Tryon and Lugardon 1991). *Phegopteris connectilis* and *P. hexagonoptera* are sister, and both feature broad folds that are elongate; both character states are reconstructed as ancestral for the genus (PL = 0.9, 1). *Phegopteris connectilis* is the only species featuring microstructure, and none feature perforations.

Plesioneuron (Blume). One of 30 species (3%) sampled. Perine morphology features thin, elongate crests and spiculate macrostructure.

Pneumatopteris Nakai. One of 80 species (1%) sampled (figs. 4*F*–4*H*, 6*C*). Spores of this diverse genus remain essentially unstudied. *Pneumatopteris truncata* is characterized by broad, echinate macrostructure with microstructure of minute crests.

Pronephrium C.Presl. Seven of 68 species (10%) sampled (figs. 4*I*–4*L*, 5*A*–5*D*). Perine morphology is highly variable in this nonmonophyletic genus (see the synonymous *Abacopteris* in Zhang 1990). The clade comprising *P. lakhimpurense* (sect. *Pronephrium*) and *P. penangianum* (sect. *Menisciopsis*) has spores with elongate, nonreticulate, broad folds, whereas the clade comprising all sampled members of section *Grypothrix* (*P. cuspidatum*, *P. simplex*, and *P. triphyllum*) differs by having spores with thin crests that may or may not be reticulate (fig. 5*A*). Based on our limited sample, all five species in section *Grypothrix* constitute a clade, and the three species represented by SEM images feature thin crests with spiculate microstructure. The ancestral states for *Pronephrium* sect. *Pronephrium* are elongate, broad folds (PL = 0.99, 0.97).

Pseudocyclosorus Ching. Three of 11 species (27%) sampled (fig. 5*E*). These three species have broad folds and conical macrostructure and lack microstructure. These characters are all ancestral for the clade (PL = 0.99, 0.95, 0.99). Grimes (1980) studied spore morphology of this genus in great detail and noted the occurrence of both cones and crests.

Pseudophegopteris Ching. Seven of 20 species (35%) sampled (fig. 5*F*). All species have identical character states of elongate and broad, reticulate folds, and these states are ancestral for the genus (PL = 1, 0.99, 0.99). Additionally, they lack microstructure and perforations (PL = 1, 0.94). This consistency reflects the long-recognized unique morphology of the genus (Holttum 1971; Wood 1973; Tryon and Lugardon 1991). Based on TEM imagery, the superficial sculpturing reflects both exospore and perine (Tryon and Lugardon 1991). An image of *P. aurita* in Wang and Dai (2010) appears appressed with no sculpturing, resembling spores of *Phegopteris decursive-pinnata*, but the image of *P. aurita* in Tryon and Lugardon (1991) is typical of the genus.

Sphaerostephanos L. Five of 185 species (3%) sampled (fig. 5*G*, 5*H*). This species-rich and morphologically diverse genus is nonmonophyletic. Our sampled taxa feature broad folds that are nonreticulate but vary in all other characters.

Stegnogramma Blume. Eight of 18 species (44%) sampled (fig. 5*I*). Spore morphology of this genus has been previously recognized as highly uniform (Wood 1973; Smith 1990; Tryon and Lugardon 1991), and our observations concur. The species

in our optimization had identical character states, and these were also reconstructed as ancestral for the genus: with broad folds (PL = 0.98) that are conical (PL = 0.97), nonreticulate (PL = 1), lack microstructure (PL = 1), and lack of perforations (PL = 1). A few curious departures, however, have been previously reported, such as *S. pilosa* from a population in Ixtlán, Oaxaca, Mexico, featuring echinae that anastomose into loops (Watkins and Farrar 2005). Our specimen of *S. pozoi* (fig. 5*I*) and the one published in Wang and Dai (2010) both have winged morphology typical of *Cyclogramma auriculata*, a member of the sister genus. *Stegnogramma pozoi* is widespread and taxonomically complex; it may include cryptic taxa with differing spore morphologies.

Steiropteris (C.Chr.) Pic. Serm. Four of 22 species (18%) sampled (fig. 5*J*). All taxa sampled in this genus feature thin crests that are elongate and reticulate (PL = 1, 1, 1), though both Smith (1980) and Tryon and Tryon (1982) note that spacing of the crests is variable. *Steiropteris* species differ in the presence of microstructure and perforations; the two species that do have microstructure both have minute crests.

Thelypteris Schmidel. Two of two species (100%) sampled. Our samples have conical, broad folds, as well as spiculate microstructure lacking perforations. Although the species *T. palustris* Schott. s.l. exhibits remarkable variation in perispore morphology across its cosmopolitan distribution, these morphologies are generally consistent within a geographic region and may represent cryptic species. The austral *T. palustris* var. *squamigera* Tardieu recognized by Tryon (1971) has an especially distinctive perispore compared with the north temperate varieties and is now recognized as a distinct species, *T. confluens* (Tryon et al. 1980).

Trigonospora Holttum. One of eight species (13%) sampled. *Trigonospora ciliata* has spores featuring conical, broad folds, spiculate microstructure, and lack of perforations. The trilete spores of this genus are unique within the family (Holttum 1971; Wagner 1974).

Discussion

Phylogenetic Analysis

Our phylogenetic results (fig. A2) are highly congruent with previous studies (Smith and Cranfill 2002; Schuettpelz and Pryer 2007; He and Zhang 2012; Almeida et al. 2016; Testo and Sundue 2016). Building on these findings, we further corroborate that many long-recognized taxa are supported by molecular phylogenetics. In particular, genera of Phegopteridoideae and the early-diverging and Neotropical clades of Thelypteridoideae are largely in accord with traditional classifications. One exception is the ACMP clade, where clades do not correspond to current generic circumscription and need further study. Another exception is the large and predominantly paleotropical christelloid clade, where many taxa are polyphyletic and will require taxonomic modifications.

Our results support the recognition of *Christella* sect. *Pelazoneuron* as a clade distinct from and widely separated from all other *Christella* (fig. A2*C*). Almeida et al. (2016) found a similar pattern with two species; our results indicate the

inclusion of five species. Our results also clearly indicate that *Pronephrium* is polyphyletic and cannot be maintained as currently circumscribed. Nonetheless, we find that the four disparate clades, none of which are sister to each other, correspond in large part to Holttum's (1982) sectional classification. The five species of section *Grypothrix*, including the type of the section, resolve together as a clade. Although the type of section *Pronephrium* is not sampled, its three constituent species are resolved as a clade. The three species in section *Menisciopsis* resolve together as a clade; however, *Chingia longissima* is nested within it. Finally, our sole representative of section *Dimorphopteris* is nested within *Pseudocyclosorus*.

Our understanding of relationships within the family will benefit from increased taxon sampling, particularly in the paleotropics, and from a phylogenomic approach (S. Fawcett, D. Barrington, M. Sundue, G. Burleigh, E. Sessa, L. Y. Kuo, A. R. Smith, unpublished manuscript). Therefore, taxonomic revisions based on the phylogeny presented in this article would be premature.

Phylogenetic Patterns of Perine Morphology

The characters with the strongest phylogenetic signal that characterize large clades are the most promising candidates for use in systematic studies. In our results, the characters reticulation and microstructure have the strongest phylogenetic signal ($P = 1.011$ e^{-15}, 5.064 e^{-13}) in the optimization, as well as high RI values (RI $= 0.71$, 0.561), suggesting low levels of homoplasy (table A1). A similar result was obtained by Haufler and Gastony (1978) and Ranker (1989), who found the characters reticulation and perforations to be useful for characterizing clades in the Cheilanthoideae (Pteridaceae). In contrast, Moran et al. (2007, 2010) did not find the character reticulation useful in characterizing clades within bolbitidoids (Dryopteridaceae). Instead, they found that the character macrostructure shape is the most useful in characterizing genera (Moran et al. 2010). These differences indicate that character utility is taxon specific and not universal between groups.

Although the characters reticulation and perforation tended to correspond well to clades, the phylogenetic patterns for other characters were more complex and homoplastic. The characters macrostructure folding and microstructure type have the lowest phylogenetic signal ($P = 1.005$ e^{-5}, 3.893 e^{-5}), as well as the lowest RI (0.39, 0.2). Microstructure is often a striking and recognizable feature of spores and quite useful for distinguishing closely related species (Tryon and Lugardon 1991; Burrows 1997; Regalado and Sanchez 2002; Nakato et al. 2004; Moran et al. 2010). Whereas Moran et al. (2010) found microstructure type of minute crests to be synapomorphic for certain clades in Dryopteridaceae, we do not find a microstructure type to be synapomorphic for any taxonomic clades, although spiculate microstructure is reconstructed with high likelihood as ancestral at backbone nodes and subclades within the cyclosoroids (fig. 7*B*). Unfortunately, microstructure can be variable within species, and the edge between states can be difficult to discern, contributing to the challenge of identifying and scoring truly independent characters representing perine morphology.

Among our characters, macrostructure form is significantly correlated with all other characters tested (table A2). This may be partly an artifact of our protocol and reflects the fact that elongate macrostructure (either broad folds or thin crests) is more likely to be reticulate or to support secondary sculpturing (microstructure or perforations) than echinae (short folds) simply because of its size.

Challenges to Scoring Character States

As with any cladistic study, assigning discrete morphological character states and assessing homology is a fundamental challenge. Although perines of different species may appear similar, they might have formed through distinct developmental pathways (Ranker 1989). The exceptional diversity within *Christella* sect. *Christella* (see Dai et al. 2002) suggests high plasticity for certain character states. Based on a detailed study of *Pseudocyclosorus* spores, Grimes (1980) proposed that crests develop through the fusion of echinae. Tryon and Lugardon (1991) suggested also that echinae may form through the dissolution of crests. Careful studies of ontogenetic sequences of spore development and perispore deposition (e.g., Haufler and Gastony 1978), along with the use of TEM imagery to elucidate internal structures (e.g., Tryon and Lugardon 1991), will inform our understanding of homology. Differences in perine morphology may be attributed to differences in the chemical composition of the sporopollenin rather than different patterns of development per se (Mitsui 1986), which represents another promising avenue of investigation.

Spore morphology is generally thought to be consistent at the species rank (Smith 1990; Tryon and Lugardon 1991), although some differences may result from imaging spores at different developmental stages (Haufler and Gastony 1978). In a few instances, however, distinct spore morphologies were noted for members of the same taxon, especially for those with broad distributions. In the case of *Thelypteris palustris*, which is nearly cosmopolitan, highly distinct spore morphologies corresponded to infraspecific taxa and/or geographic regions (Tryon 1971; Tryon et al. 1980). Widespread species with striking differences in morphology among published images include *Pseudophegopteris aurita*, *Cyclosorus interruptus*, and *Stegnogramma pozoi* (Tryon and Lugardon 1991; Wang and Dai 2010). These differences may be indicative of unrecognized cryptic diversity, as was shown for the *Coryphopteris japonica* complex (Nakato et al. 2004), with spores exhibiting perine morphologies that were echinate (diploid), broad folds (triploid), or thin crests (tetraploid).

Conclusions

The goal of this work is to examine spore morphological evolution in a phylogenetic context and to determine the extent to which it corroborates current taxonomic concepts in the Thelypteridaceae. We find that spore traits can be informative at multiple taxonomic ranks, from subfamily to species. Characters pertaining to macrostructure and perforations, in particular, were reconstructed as synapomorphic for genera or infrageneric taxa in the Thelypteridaceae. We

find that spores of certain genera, such as *Amauropelta* and *Stegnogramma*, exhibit uniform morphology, whereas others such as *Christella* sect. *Christella* are heterogeneous and defy characterization. This high variability of perine characters within the christelloid clade suggests that it is a promising group on which to focus further sampling. Perine morphology also acts as an indicator that something might be incorrectly identified or classified when it appears to be in conflict with that of near relatives. Finally, we demonstrate that the repository of high-quality SEM images of spores in the literature serves as a rich source of morphological data. Accordingly, future phylogenetic studies of pteridophytes should incorporate perine morphology characters in conjunction with other data.

Literature Cited

Ackerman JD 2000 Abiotic pollen and pollination: ecological, functional, and evolutionary perspectives. Plant Syst Evol 222:167–185.

Almeida TE, S Hennequin, H Schneider, AR Smith, JAN Batista, AJ Ramalho, K Proite, A Salino 2016 Towards a phylogenetic generic classification of Thelypteridaceae: additional sampling suggests alterations of neotropical taxa and further study of paleotropical genera. Mol Phylogenet Evol 94:688–700.

Alvarez-Fuentes O 2010 The systematics of the genus *Amauropelta* (Pteridophyta: Thelypteridaceae) in the Caribbean islands. PhD diss. Michigan State University, East Lansing.

Bernard S, K Benzerara, O Beyssac, N Menguy, F Guyot, GE Brown Jr, B Goffé 2007 Exceptional preservation of fossil plant spores in high-pressure metamorphic rocks. Earth Planet Sci Lett 262:257–272.

Bolick MR 1978 Taxonomic, evolutionary, and functional considerations of Compositae pollen ultrastructure and sculpture. Plant Syst Evol 130:209–218.

Brown CA 1960 What is the role of spores in fern taxonomy? Am Fern J 50:6–14.

Burrows JE 1997 The use of spore morphology as a taxonomic tool in the delimitation of the Southern African species of *Ophioglossum* L. (Ophioglossaceae: Pteridophyta). Pages 43–65 *in* Holttum memorial volume: published to commemorate the centenary of the birth of Professor R. E. Holttum. Royal Botanic Gardens, Kew.

Carrión JS, MJ Cano, J Guerra 1995 Spore morphology in the moss genus *Pterygoneurum* Jur. (Pottiaceae). Nova Hedwig 61:481–496.

Chao YS, YM Huang 2018 Spore morphology and its systematic implication in *Pteris* (Pteridaceae). PLoS ONE 13:p.e0207712.

Crepet WL 1996 Timing in the evolution of derived floral characters: Upper Cretaceous (Turonian) taxa with tricolpate and tricolpate-derived pollen. Rev Palaeobot Palynol 90:339–359.

Dai S, Q Wang, W Bao, K Shing 2002 Spore morphology of pteridophytes from China: Thelypteridaceae. Acta Phytotaxon Sin 40:334–344.

Dai S, Q Wang, W Bao, X Zhang, D Zhang 2005 Spore morphology of pteridophytes from China. IV. Thelypteridaceae 2. Acta Phytotaxon Sin 43:233–245.

Edgar RC 2010 Search and clustering orders of magnitude faster than BLAST. Bioinformatics 26:2460–2461.

Fawcett S 2018 *Coryphopteris simulata* (Thelypteridaceae), a new combination for the Massachussetts fern. Am Fern J 108:107–112.

Ferguson IK 1984 Pollen morphology and biosystematics of the subfamily Papilionoideae (Leguminosae). Plant Biosyst 2:377–394.

Ferguson IK, MM Harley 1993 The significance of new and recent work on pollen morphology in the Palmae. Kew Bull 48:205–243.

Fernandes RS, JC Yesilyurt, A Salino 2014 New species and combinations in *Meniscium* (Thelypteridaceae). Phytotaxa 184:1–11.

Ferrarini E, F Ciampolini, REG Pichi Sermolli, D Marchetti 1986 Iconographia palynologica pteridophytorum Italiae. Webbia 40:1–201.

Freyman WA 2015 SUMAC: constructing phylogenetic supermatrices and assessing partially decisive taxon coverage. Evol Bioinform 11: EBO-S35384.

Furness CA, PJ Rudall 2004 Pollen aperture evolution—a crucial factor for eudicot success? Trends Plant Sci 9:154–158.

Grimes JW 1980 Spore morphology in Thelypteridaceae. I. *Pseudocyclosorus*. Kew Bull 34:517–520.

Harmon LJ, JT Weir, CD Brock, RE Glor, W Challenger 2007 GEIGER: investigating evolutionary radiations. Bioinformatics 24:129–131.

Haufler CH, GJ Gastony 1978 Systematic implications of spore morphology in *Bommeria* and related fern genera. Syst Bot 1:241–256.

He LJ, XC Zhang 2012 Exploring generic delimitation within the fern family Thelypteridaceae. Mol Phylogenet Evol 65:757–764.

Hickey RJ 1986 *Isoëtes* megaspore surface morphology: nomenclature, variation, and systematic importance. Am Fern J 76:1–16.

Holttum RE 1971 Studies in the family Thelypteridaceae. III. A new system of genera in the Old World. Blumea 19:17–52.

——— 1974 Thelypteridaceae of Africa and adjacent islands. J S Afr Bot 40:123–168.

——— 1982 Thelypteridaceae. Flora Males II 1:334–560.

Huang TC 1981 Spore flora of Taiwan (Pteridophyta). National Taiwan University, Taipei.

Huelsenbeck JP, F Ronquist 2001 MRBAYES: Bayesian inference of phylogenetic trees. Bioinformatics 17:754–755.

Joaquin CC, PM Zamora 1996 Diversity of spores in Philippine ferns. University of the Philippines, Center for Integrative and Development Studies, Biodiversity Conservation Program, Quezon City.

Katoh K, J Rozewicki, KD Yamada 2017 MAFFT online service: multiple sequence alignment, interactive sequence choice and visualization. Brief Bioinform, https://doi.org/10.1093/bib/bbx108.

Kearse M, R Moir, A Wilson, S Stones-Havas, M Cheung, S Sturrock, S Buxton, A Cooper, S Markowitz, C Duran 2012 Geneious Basic: an integrated and extendable desktop software platform for the organization and analysis of sequence data. Bioinformatics 28:1647–1649.

Kenrick P, PR Crane 1997 The origin and early diversification of land plants. Vol 560. Smithsonian Institution, Washington, DC.

Kosenko VN 1999 Contributions to the pollen morphology and taxonomy of the Liliaceae. Grana 38:20–30.

Kott L, DM Britton 1983 Spore morphology and taxonomy of *Isoëtes* in northeastern North America. Can J Bot 61:3140–3163.

Kramer KU, PS Green 1990 Pteridophytes and gymnosperms. Pages 263–272 *in* K Kubitski, ed. The families and genera of vascular plants. Vol 1. Springer, Berlin.

Lanfear R, PB Frandsen, AM Wright, T Senfeld, B Calcott 2016 PartitionFinder 2: new methods for selecting partitioned models

of evolution for molecular and morphological phylogenetic analyses. Mol Biol Evol 34:772–773.

Lewis PD, JS Harvey, EM Waters, DOF Skibinski, JM Parry 2001 Spontaneous mutation spectra in supF: comparative analysis of mammalian cell line base substitution spectra. Mutagenesis 16: 503–515.

Little DP, DS Barrington 2003 Major evolutionary events in the origin and diversification of the fern genus *Polystichum* (Dryopteridaceae). Am J Bot 90:508–514.

Lloyd RM, EJ Klekowski Jr 1970 Spore germination and viability in Pteridophyta: evolutionary significance of chlorophyllous spores. Biotropica 2:129–137.

Miller MA, W Pfeiffer, T Schwartz 2010 Creating the CIPRES Science Gateway for inference of large phylogenetic trees. Pages 1–8 *in* Gateway Computing Environments Workshop (GCE), New Orleans, LA, November 14, 2010. IEEE.

Mitsui K 1986 The development of the perispore in the fern family Thelypteridaceae. Pages 401–403 *in* S Blackmore, IK Ferguson, eds. Pollen and spores: form and function. Academic Press, London.

Mitui K 1982 Spore morphology of Japanese ferns. Toyojyou, Tokyo.

Moon SM, BY Sun 2008 Spore morphology of Korean Thelypteridaceae. Korean J Plant Taxon 38:459–476.

Moran RC, JG Hanks, PH Labiak 2018 Evolution of spore morphology in the Blechnaceae. Int J Plant Sci 179:712–729.

Moran RC, JG Hanks, P Labiak, M Sundue 2010 Perine morphology of bolbitidoid ferns (Dryopteridaceae) in relation to phylogeny. Int J Plant Sci 171:872–881.

Moran RC, JG Hanks, G Rouhan 2007 Spore morphology in relation to phylogeny in the fern genus *Elaphoglossum* (Dryopteridaceae). Int J Plant Sci 168:905–929.

Morton CV 1963 Some West Indian species of *Thelypteris*. Am Fern J 53:57–70.

Moy CJ 1988 Variations of fern spore ultrastructure as reflections of their evolution. Grana 27:39–51.

Nakato N, N Sahashi, M Kato 2004 Cytotaxonomy of the *Thelypteris japonica* complex (Thelypteridaceae). Acta Phytotaxon Geobot 55: 89–105.

Pagel M 1994 Detecting correlated evolution on phylogenies: a general method for the comparative analysis of discrete characters. Proc R Soc B 255:37–45.

Paolillo DJ Jr, LB Kass 1977 The relationship between cell size and chloroplast number in the spores of a moss, *Polytrichum*. J Exp Bot 28:457–467.

Pichi Sermolli REG 1977 Tentamen Pteridophytorum genera in taxonomicum ordinem redigendi. Webbia 31:313–512.

Poole MM, DR Hunt 1980 Pollen morphology and the taxonomy of the Commelinaceae: an exploratory survey. VIII. American Commelinaceae. Kew Bull 34:639–660.

Porebski S, LG Bailey, BR Baum 1997 Modification of a CTAB DNA extraction protocol for plants containing high polysaccharide and polyphenol components. Plant Mol Biol Rep 15:8–15.

PPG (Pteridophyte Phylogeny Group) I 2016 A community-derived classification for extant lycophytes and ferns. J Syst Evol 54:563–603.

Puttock CF, CJ Quinn 1980 Perine morphology and the taxonomy of the Australian Aspleniaceae. Aust J Bot 28:305–322.

Rambaut A, MA Suchard, D Xie, AJ Drummond 2015 Tracer version 1.6. http://tree.bio.ed.ac.uk/software/tracer/.

Ranker TA 1989 Spore morphology and generic delimitation of new world *Hemionitis*, *Gymnopteris*, and *Bommeria* (Adiantaceae). Am J Bot 76:297–306.

Regalado L, C Sánchez 2002 Spore morphology as a taxonomic tool in the delimitation of three *Asplenium* L. species complexes (Aspleniaceae: Pteridophyta) in Cuba. Grana 41:107–113.

Rothfels CL, A Larsson, LY Kuo, P Korall, WL Chiou, KM Pryer 2012 Overcoming deep roots, fast rates, and short internodes to resolve the ancient rapid radiation of eupolypod II ferns. Syst Biol 61:490–509.

Schneider H, AR Schmidt, J Heinrichs 2016 Burmese amber fossils bridge the gap in the Cretaceous record of polypod ferns. Perspect Plant Ecol Evol Syst 18:70–78.

Schuettpelz E, KM Pryer 2007 Fern phylogeny inferred from 400 leptosporangiate species and three plastid genes. Taxon 56:1037–1037.

Shah SN, M Ahmad, M Zafar, F Ullah, W Zaman, K Malik, N Rashid, S Gul 2019 Taxonomic importance of spore morphology in Thelypteridaceae from northern Pakistan. Microsc Res Tech 82:1326–1333. https://doi.org/10.1002/jemt.23283.

Smith AR 1971 Systematics of the neotropical species of *Thelypteris* section *Cyclosorus*. Univ Calif Publ Bot 59:1–136.

——— 1974 A revised classification of *Thelypteris* subgenus *Amauropelta*. Am Fern J 64:83–95.

——— 1980 Taxonomy of *Thelypteris* subgenus *Steiropteris*, including *Glaphyropteris* (Pteridophyta). Univ Calif Publ Bot 76:1–38.

——— 1990 Thelypteridaceae. Pages 263–272 *in* K Kubitski, ed. The families and genera of vascular plants: pteridophytes and gymnosperms. Springer, Berlin.

Smith AR, R Cranfill 2002 Intrafamilial relationships of the thelypteroid ferns (Thelypteridaceae). Am Fern J 92:131–149.

Smith AR, KM Pryer, E Schuettpelz, P Korall, H Schneider, PG Wolf 2006 A classification for extant ferns. Taxon 55:705–731.

——— 2008 Fern classification. Pages 417–467 *in* TA Ranker, CH Haufler, eds. Biology and evolution of ferns and lycophytes. Cambridge University Press, Cambridge.

Stamatakis A 2014 RAxML version 8: a tool for phylogenetic analysis and post-analysis of large phylogenies. Bioinformatics 30:1312–1313.

Sundue M, A Vasco, RC Moran 2011 Cryptochlorophyllous spores in ferns: nongreen spores that contain chlorophyll. Int J Plant Sci 172:1110–1119.

Taberlet P, L Gielly, G Pautou, J Bouvet 1991 Universal primers for amplification of three non-coding regions of chloroplast DNA. Plant Mol Biol 17:1105–1109.

Testo W, M Sundue 2016 A 4000-species dataset provides new insight into the evolution of ferns. Mol Phylogenet Evol 105:200–211.

Tryon AF 1971 Structure and variation in spores of *Thelypteris palustris*. Rhodora 73:444–460.

Tryon AF, B Lugardon 1991 Spores of the Pteridophyta. Springer, New York.

Tryon AF, R Tryon, F Badré 1980 Classification, spores, and nomenclature of the marsh fern. Rhodora 82:461–474.

Tryon R, AF Tryon 1982 Ferns and allied plants with special reference to tropical America. Springer, New York.

Vaarama A 1953 Some chromosome numbers of Californian and Finnish moss species. Bryologist 56:169–177.

Van Bergen PF, ME Collinson, DEG Briggs, JW De Leeuw, AC Scott, RP Evershed, P Finch 1995 Resistant biomacromolecules in the fossil record. Acta Bot Neerl 44:319–342.

Vasco A, RC Moran, G Rouhan 2009 Monograph of the *Elaphoglossum ciliatum* group (Dryopteridaceae). Brittonia 61:241–272.

Wagner WH 1974 Structure of spores in relation to fern phylogeny. Ann Mo Bot Gard 61:332–353.

Wallace S, A Fleming, CH Wellman, DJ Beerling 2011 Evolutionary development of the plant spore and pollen wall. AoB Plants, https://doi.org/10.1093/aobpla/plr027.

Wang H, RR Mill, S Blackmore 2003 Pollen morphology and infrageneric evolutionary relationships in some Chinese species of *Pedicularis* (Scrophulariaceae). Plant Syst Evol 237:1–17.

Wang QX, XL Dai 2010 Spores of Polypodiales (Filicales) from China. Science, Beijing.

Wang RX, W Shao, L Liu, J Liu, XC Deng, SG Lu 2015 A systematic study of the fern genus *Mesopteris* Ching (Thelypteridaceae). Am Fern J 105:11–19.

Watkins JE, D Farrar 2005 Origin and taxonomic affinities of *Thelypteris* (subgen. *Stegnogramma*) *burksiorum* (Thelypteridaceae) Brittonia 57:183–201.

Wei LL, SY Dong 2012 Taxonomic studies on *Asplenium* sect. *Thamnopteris* (Aspleniaceae). II. Spore morphology. Nord J Bot 30:90–103.

Wiens JJ, MC Morrill 2011 Missing data in phylogenetic analysis: reconciling results from simulations and empirical data. Syst Biol 60:719–731.

Wood C 1973 Spore variation in the Thelypteridaceae. Pages 191–202 *in* AC Jermy, JA Crabbe, BA Thomas, eds. The phylogeny and classification of the ferns. Academic Press, London.

Zhang JT 1976 Sporae pteridophytorum sinicorum. Science, Beijing.

Zhang Y 1990 Spore morphology of Chinese pteridophytes. Science, Beijing.